ANALYSIS OF XENON-INDUCED POWER OSCILLATIONS IN AN INTEGRAL PRESSURIZED WATER REACTOR USING MCNP CODE COUPLED WITH SINGLE CHANNEL THERMAL FEEDBACK

A Thesis

by

EDWIN AMANDA CRYSTAL

Submitted to the Office of Graduate and Professional Studies of
Texas A&M University
in partial fulfillment of the requirements for the degree of

MASTER OF SCIENCE

Chair of Committee,	Sunil Chirayath
Committee Members,	John Ford
	Rupak Mahapatra
Head of Department,	Michael Nastasi

May 2021

Major Subject: Nuclear Engineering

ABSTRACT

Nuclear energy is an attractive source of energy because it decreases our dependence on fossil fuels. Emission of greenhouse gases by burning fossil fuels and the limited supply of oil, gas, and coal, makes nuclear energy an attractive alternative to carbon-based fuels. Nuclear fuel contains much more energy than a equivalent mass of hydrocarbons or coal, hence making it a reliable energy resource. The advanced small modular reactors come with improved safety through various design features such as lower fuel inventory, passive heat removal systems, reduced length of large core cooling piping, etc. The smaller physical size contributes to added flexibilities in fabrication, construction, lower capital cost and shorter construction time contribute to reduced investment risks.

The main objective of this study is to assess xenon-induced power oscillations in a generic small modular reactor (SMR) of the integral pressurized water reactor (*i*PWR) type. The Monte Carlo neutronics code MCNP is used to model the reactor core and carry out the fuel irradiation simulations. The goal is to develop a methodology for analyzing the dynamic phenomenon of xenon-induced power oscillation by coupling MCNP with a thermal feedback algorithm characterizing the temperature effects using a single fuel-coolant channel. A multi-physics coupling algorithm developed will incorporate the effect of thermal-hydraulic feedback (temperature dependent neutron cross-section of fuel and change in axial coolant density) on xenon-oscillation phenomenon induced by a neutron reactivity change in the reactor core. Establishing

high fidelity thermal-neutronics coupled methodologies are important for analyzing reactor transients featuring significant variations in localized neutron flux.

ACKNOWLEDGEMENTS

I would like to thank my Committee Chair, Dr Sunil S. Chirayath for always being available, giving insights and guidance in all aspects of the research and providing an environment where I have grown and matured upon arriving at Texas A&M University. He is an excellent academic, and a true gentleman.

I want to thank my Committee Members, Dr. John Ford and Dr. Rupak Mahapatra, for their support throughout the course of this research.

Thanks to my friends and colleagues and the Nuclear Engineering department faculty and staff at Texas A&M University for making my time there a greatly rewarding one.

Finally, thanks to my family and loved ones for their encouragement, friendship, and love.

CONTRIBUTORS AND FUNDING SOURCES

Contributors

This work was supervised by a thesis committee consisting of Dr. Sunil Chirayarh [advisor and committee chair] and Dr. John Ford of the Department of Nuclear Engineering and Dr. Rupak Mahapatra of the Department of Physics.

Funding Sources

Graduate study was supported by Graduate Research Assistantship from Texas A&M Engineering Experiment Station, Texas A&M University.

NOMENCLATURE

***i*PWR**	Integral Pressurized Water Reactor
LWR	Light Water Reactor
LOCA	Loss of Coolant Accident
LEU	Low Enriched Uranium
PWR	Pressurized Water Reactor
SCA	Single Channel Analysis
SMR	Small Modular Reactor
IAEA	International Atomic Energy Agency
MCNP	Monte Carlo N- Particle Transport Code
BAR	Burnable Absorber Rod

TABLE OF CONTENTS

Page

ABSTRACT……. ii

ACKNOWLEDGEMENTS…….. iv

NOMENCLATURE…….. vi

TABLE OF CONTENTS…….. vii

LIST OF FIGURES……..... ix

LIST OF TABLES…… xi

1 INTRODUCTION…… 1

1.1 Thesis Objective…… 1
1.2 Background……..... 2
1.3 Previous Work……..... 4

2 LITERATURE REVIEW…… 5

2.1 Small Modular Reactors……. 5
2.2 Pressurized Water Reactors……. 6
2.3 Integral Pressurized Water Rectors……. 7
2.4 Existing *I*pwr Smr Designs……..... 8
2.4.1 Holtec Smr Design……..... 8
2.4.2 Nuscale Smr Design……..... 9
2.4.3 Westington Smr……..... 9
2.4.4 B&W Mpower Smr…… 9
2.5 Description Of Xenon Oscillation Phenomenon…… 10
2.5.1 Axial Xenon Oscillation……..... 13
2.6 Simulation Approach……..... 14

3 METHODOLOGY……. 16

3.1 Coupling Scheme……..... 16
3.2 Single Channel Analysis For Thermal Analysis…….. 19

3.3 Description Of Tools…… 21
3.3.1 Mcnp……..... 21
3.3.2 Cinder 90 For Fuel Depletion…….. 23

4 REACTOR DESIGN…….. 25

4.1 Existing Pwr Assembly Parameters……..... 25
4.2 Fuel Enrichment……... 26
4.3 Reactivity Control……..... 28
4.4 Smr Core Model Using Mcnp…….. 29
4.5 Burnable Absorber Rod…… 31
4.5.1 Methods For Excess Reactivity Control…….. 31
4.5.2 Implications Of Boron Free Coolant In Smr Operations……. 32

5 RESULTS AND DISCUSSION……. 34

5.1 Effective Neutron Multiplication Factor And Fuel Burn Up…… 34
5.2 Xenon Stability Results……..... 46

6 CONCLUSION…… 50

6.1 Research Summary…… 50
6.2 Future Research……. 51

LIST OF FIGURES

Figure		Page
1	Traditional PWR versus B&W mPower Reactor; The Babcock & Wicox Company 2011…….	8
2	Production scheme of Xe-135 in nuclear fission…….....	11
3	Time dependence of ^{135}Xe concentration following power-level changes…….....	12
4	Axial xenon oscillation with axial profiles of nuclear reactor neutron flux (ϕ) and xenon concentration…….....	13
5	A system level flowchart of the developed multi-physics coupling routine……..	18
6	Axial Temperature variation of fuel, cladding and coolant with respect to fuel height…….....	21
7	Radial PWR Fuel Pin Geometry of the SMR design……..	25
8	Axial cross section of a single fuel assembly……..	26
10(a)	Radial Cross Section of the SMR core Model geometry……	27
10(b)	Radial Cross section of the burnable absorber rod (BAR)……..	27
11	Radial Cross Section of SMR Model (Assemblies Numbered.....	29
12	Axial Cross Section of SMR Model (Fuel Regions Visible….....	30

13	Plot of Effective multiplication factor vs time in days…….....	35
14	SMR Xenon Mass vs Burnup of the fuel…….	36
15	Plot of Volumetric Heat generation rate with Height of the fuel at steady state……..	37
16	Temperature Profile of Fuel, Cladding inner and outer and Coolant in the core……...	39
17	Evolution of Axial temperature profile of fuel…….....	40
18	Evolution of Volumetric heat generation rate in the fuel with burnup……	41
19	Evolution of Axial Bulk Coolant temperature in the SMR core model…….....	41
20	Evolution of Fuel, cladding and coolant temperatures for fuel depletion convergence calculation……..	45
21	Buildup of Xenon mass with cumulative burn up of the fuel in SMR core……	47
22	Xenon Oscillatory behavior with removal of control rod…….....	47
23	Xenon Oscillatory behavior with the Control Rod Movement.....	48
24	Xenon Oscillations with Cumulative Burn up…….	49

LIST OF TABLES

Figure		Page
1	PWR Fuel Assembly Details Used for the SMR Assembly……..	30
2	Temperature dependent neutron cross section extensions……..	43
3	Effective Multiplication Factor for fuel depletion convergence….	44

CHAPTER I

INTRODUCTION

1.1 Thesis Objective

The main objective of this study is to assess xenon-induced power oscillations in a generic small modular reactor (SMR) of the integral pressurized water reactor (*i*PWR) type. The goal is analyze the dynamic phenomenon of xenon-induced power oscillation in the reactor core, as closely as possible, using the Monte Carlo N- Particle neutronics code (MCNP) by coupling it with a thermal feedback algorithm characterizing a single fuel-coolant channel. A multi-physics coupling algorithm developed will incorporate the effect of thermal-hydraulic feedback (temperature dependent neutron cross-section of fuel and change in axial coolant density) on xenon-oscillation phenomenon induced by a neutron reactivity change in the reactor core. Establishing high fidelity thermal-neutronics coupled methodologies are important for analyzing reactor transients featuring significant variations in localized neutron flux.

In this work, an *i*PWR type SMR is analyzed from neutronics and thermal-hydraulics perspectives. Height to diameter ratio of the SMR is 1.23 due to which the xenon induced power oscillations are more pronounced. The Monte Carlo radiation transport code, MCNP6.2 [1] is used to perform neutronics simulations for analyzing xenon-oscillation phenomenon and a new algorithm is developed for coupling thermal-hydraulic feedback to neutronics for better analyzing the xenon-oscillation.

1.2 Background

Demand of energy will increase substantially over the coming years due to the growth in the world's population and economy, coupled with rapid urbanization. The challenge of meeting rapidly growing energy demand, whilst reducing harmful emissions of greenhouse gases, is attainable. Increased electrification of end-uses such as transport, space cooling, large appliances, and others are key contributors to rising electricity demand. Aside from the challenges of meeting increased demand and reducing greenhouse gas emissions, cleaner air is a vital need.

Studies have repeatedly shown that nuclear energy is a low-carbon-emitting source of electricity production. It is among one of the lowest carbon dioxide emitting electricity generation technology per unit of energy produced when considering total life-cycle emissions [2]. It is the second largest source of low-carbon electricity production globally (after hydropower) and provided about 30% of all low-carbon electricity generated in 2017. Almost all reports on future energy supply from major organizations suggest an expanded role for nuclear power is required, alongside growth in other forms of low-carbon power generation, to create a sustainable future energy system. A major two-year study by the Massachusetts Institute of Technology Energy Initiative (MITEI) published in September 2018 [2] underlined the pressing need to increase nuclear power generation worldwide.

Apart from the public opinion, sensibility related to plant safety and waste disposal issues, the economic evaluation from investors and utilities must also be taken into consideration by the nuclear industry. Smaller nuclear reactors were instrumental in

commercial nuclear power to facilitate the development and demonstration of early reactor technologies [3]. SMRs have attractive characteristics of simplicity, enhanced safety, and require limited financial resources [3]. SMRs have proven to be a viable solution to overcome electrical grids with limited capacity, remote areas requiring smaller and localized power centers, to avoid long and expensive transmission lines, financial capabilities, which preclude raising the huge capitals required by light water reactors (LWRs).

The use of the Monte Carlo method in core modeling and reactor physics simulations have become increasingly popular to capture the complex core geometries and material heterogeneity featured in advanced reactor designs [1]. This trend has been aided and even accelerated by ever increasing computational power through increased computer memory capacity and processor speeds [4].

As such, for this study, a generic SMR design of *i*PWR type was modeled and analyzed. A multi-physics coupling routine was developed and utilized to introduce thermal hydraulic assessment and feedback in the form of temperature-dependent neutron interaction cross-section of the fuel, specifically uranium and reactor core coolant density. The threat to safety and operation of the generic SMR model posed by xenon-induced power oscillations were assessed in this research. The goal was to develop a methodology whereby a dynamic phenomenon such as xenon-induced power oscillations could be analyzed using the Monte Carlo neutronics analysis method whilst informing design and development of SMR technology.

1.3 Previous Work

The growing interest to deploy SMR technology requires a substantial amount of R&D for verifying their safety characteristics. High-fidelity computational models (neutronics and thermal hydraulic), simulations, and analyses support this R&D mission. Although coupled neutron kinetics and thermal hydraulics methodologies exist and have been extensively used with respect to the PWR designs and other light water applications, there is limited work done for iPWR-type SMRs using such simulation approaches [5]. There have been studies with respect to the xenon-induced power oscillations [6] but the study was limited to Single Channel Analysis (SCA) as far as thermal hydraulics aspects are concerned. The current research is extended to perform single-channel thermal feedback and multi-physics analysis of the reactor core neutronics and the fission heat generation. The SIGACE code was used to produce Doppler broadened neutron interaction cross-sections for the nuclides deemed important to the 2012 study [6]. In this research all neutron cross-sections are appropriately treated to fully implement the effect of temperature on the location specific fuel material by evaluating the weighted fractions of temperature dependent neutron cross-sections [7]. Additionally, in this research work, the change in reactivity is observed and evaluated for convergence for each time step. The change in reactivity in two consecutive convergence steps with the change in water density and temperature dependent weighted fractions of fuel ($\Delta\rho \leq 10$mK) is less than or equal to 10 milli K is the convergence criteria.

CHAPTER II

LITERATURE REVIEW

2.1 Small Modular Reactors (SMRs)

Smaller size nuclear reactors can represent a viable solution for developing countries, countries without a large electrical grid infrastructure, and for developed countries when limitation on capital at risk applies [5]. According to the IAEA definition, small modular reactors are reactors producing power less than 300MWe [8]. Small and medium sized rectors or modular reactors are increasing due to extended power flexibility, enhanced safety which includes both inherent and passive safety. IAEA member states, defines small reactors as reactors having rated electrical power of less than 300 MWe or thermal output of less than 1000 MWt, while medium reactors are from 300 to a maximum of 700 MWe. Alternatives and favorable circumstances are thought while planning deliberately SMRs making the reactors small. Under this characterization there are many existing reactor designs that could be named SMRs. SMRs utilize their size for their benefit to accomplish this design objective. These reactors stress safety, security, and cost.

In deliberately small sized reactors, an example of safety would be the decreased thermal power density of the core allowing for passive heat removal systems by natural circulation during all accident scenarios eliminating the need for forced circulation pumps. These are indispensable components of the safety systems employed by existing small reactor designs [5].

Another design option achievable by having a deliberately small reactor is placing the entire reactor containment underground. This leads to an additional barrier for the radiation source term in the case of a radioactive release, a safety benefit. This also provides additional protection from missile strikes and aircraft impact, a security benefit. These and other aspects all point to decreased costs as system components are eliminated for simpler systems driven by physical phenomena and plant safety and security.

The primary cost advantage of the deployment of SMRs is the reduced up-front capital costs to the developer. SMRs will have relatively low capital costs and the ability to meet a larger range of applications from base loads in high demand areas to implementation in developing and emerging grids incompatible to large 1000MWe reactors [5]. Modularity benefits such as standardized core components that can be manufactured in a factory setting result in increased quality assurance and decreased plant construction times. SMRs have been shown to be economically competitive with larger power reactors [3].

The unconventional physical dimensions of SMRs calls for neutronics and thermal-hydraulics analysis, especially the reactor transient behavior. For example, to prevent loss of coolant accident scenario long coolant pipes are avoided by placing pressurizer, steam generator, coolant pumps, etc., in the reactor vessel itself unlike large Pressurized Water Reactors (PWRs).

2.2 Pressurized water reactor

A PWR is a light water reactor. It operates with a thermal neutron spectrum. The primary coolant for the reactor is light water, which also acts as the moderator. The fuel is uranium dioxide (UO_2) or mixed oxide containing both uranium dioxide and plutonium dioxide (UO_2+PuO_2). usually with low enriched uranium (LEU). By keeping the reactor pressurized, the coolant is kept from boiling and remains in single phase as a liquid despite the high temperatures (~300°C)

The primary coolant is maintained at pressures in the region of ~15MPa by the pressurizer. Typical PWR power plants also use light water as the secondary coolant which passes through the steam generator producing super-heated steam to drive the turbine and produce electricity. The 4-loop PWR has four steam generators connected to one reactor core and one pressurizer with a coolant pump for each loop**.**

2.3 Integral Pressurized Water Reactors

In a PWR, one of the major accidents is the loss of coolant accident or a large-break LOCA. In this accident, one of the large coolant pipes connecting the reactor core to the steam generators undergoes a double ended break leading to rapid uncover of the core and a large fraction of the coolant inventory would be lost, that could lead to the melting of fuel assemblies. This LOCA could lead to a large-scale radioactive fission source term release. Hence, in the case of the large-break LOCA, a plethora of auxiliary safety systems have to be added to the design to ensure that the core is covered with coolant and heat removal systems remains capable of removing the remaining decay heat. The Integral Pressurized Water Reactor (*i*PWR) takes a excellent approach in

curbing this accident scenario. The *i*PWR design places the pressurizer, steam generator and coolant pump along with the core inside the same pressure vessel. Thus, eliminating the need for long coolant pipes and the associated possibility of a large-break LOCA altogether. This can be done only in the case of SMRs as their smaller size and associated components makes forging a large enough pressure vessel possible. The proposed SMRs that are near deployment are all this *i*PWR type. These SMR designs not only eliminate an entire category of accident scenarios but also increase the coolant inventory in the core allowing heat removal by natural circulation to be applicable over a wider range of operation. It is this efficient and inherent safe design that symbolizes SMRs. In this research the SMR to be investigated will be of the *i*PWR type with a component layout envisioned to be similar to that of the mPower shown in Figure 1 [9].Smaller reactors allow a pressure vessel large enough to accommodate the required components to be forged.

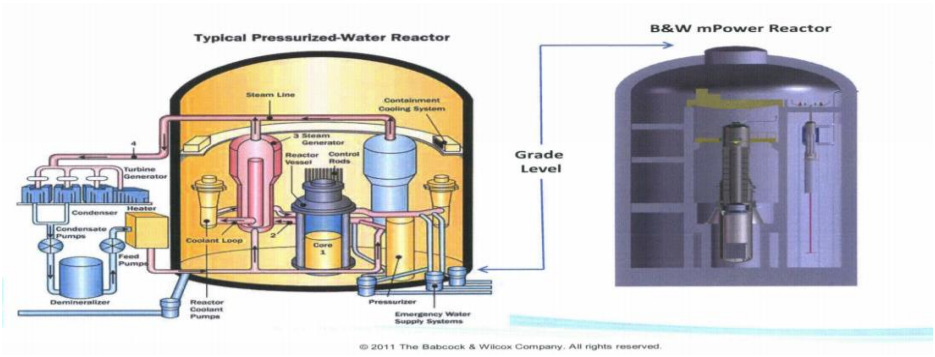

Figure 1: Traditional PWR versus B&W mPower Reactor; The Babcock & Wicox Company 2011

Reprinted from mpower Reactor Design Overview Workshop Slides NRC,2011, www.nrc.gov [9]

2.4 Exciting *i*PWR SMR designs

2.4.1 Holtec SMR design

The Holtec SMR-160 is an *i*PWR design offered by SMR LLC, a subsidiary company of Holtec International (Holtec). SMR 160 does not rely on any pumps or motors to remove heat from nuclear fuel during any accident scenario. Power of the reactor is 160MWe. The reactor safety system is passive and for all performance modes, natural circulation is used. All safety systems of the plant exist inside containment and are protected further by the concrete enclosure structure. [10]

2.4.2 NuScale SMR

The design of NuScale SMR is developed at Oregon State University. NuScale is a natural circulation light water reactor with the reactor core and helical coil steam generators located in a common reactor vessel in a cylindrical steel containment. The reactor vessel containment module is submerged in water in the reactor building safety related pool, which is also the ultimate heat sink for the reactor. The pool portion of the reactor building is located below grade. [11]

2.4.3 Westinghouse SMR

The Westinghouse SMR is a >225 MWe is also an *i*PWR-type design with all primary components located inside the reactor vessel. The safety system is passive. Passive safety features designed to shut the plant down automatically and keep it cool without human intervention or AC power. Reduced fuel, resulting in reduced radioactivity amounts released in the case of an accident. Passive heat removal with on-

site water inventory, which relies on the natural forces of evaporation, condensation, and gravity. [12]

2.4.4 B&W mPower SMR

The B&W mPower SMR is an *i*PWR design offered by Generation mPower LLC, a subsidiary company of Babcock & Wilcox (B&W). The design is derived from B&W's reactor technology and represents the culmination of existing B&W generation III+ technology. Th reactor is cooled by forced cooling technique. Pressure vessel houses the core, coolant pumps, pressurizer, and steam generator. The reactor building is below grade. The power of each module is 180 MWe. To mimic the existing large PWRs, a plant configuration featuring 10 modules at a single site would result in a total power of 1800 MWe. The fuel height is of the form of reduced height standard PWR 17 x 17 fuel assemblies with a maximum fuel enrichment of 5.0 wt. % ^{235}U on a nominal four-year refueling cycle. [13]

2.5 Description of Xenon Oscillation Phenomenon

Xenon-135 (^{135}Xe) is one of the nuclear fission product isotopes. Xe-135 is a strong neutron "poison" [14] [15] and hence plays a key role in the neutronics of the reactor core. Xe-135 has a very large thermal neutron absorption cross section (2.6 million barns) and has a relatively high cumulative fission yield of approximately six percent [15].

A simplified production scheme of Xe-135 [16] is shown in Figure-3. The direct fission yield of Xe-135 is only 0.25 percent with the remainder of production is from the decay of its precursors; antimony-135 (Sb-135), tellurium-135 (Te-135) and iodine-135

(I-135). The half-lives of the decay of Sb-135 to Te-135 and Te-135 to I-135 are very short (1.7 s and 19 s, respectively). However, I-135 decays to Xe-135 with a half-life of 6.6 hours. Hence, Xe-135 is mainly produced with a delay while its removal is based on its large neutron absorption cross section and its own decay [16].

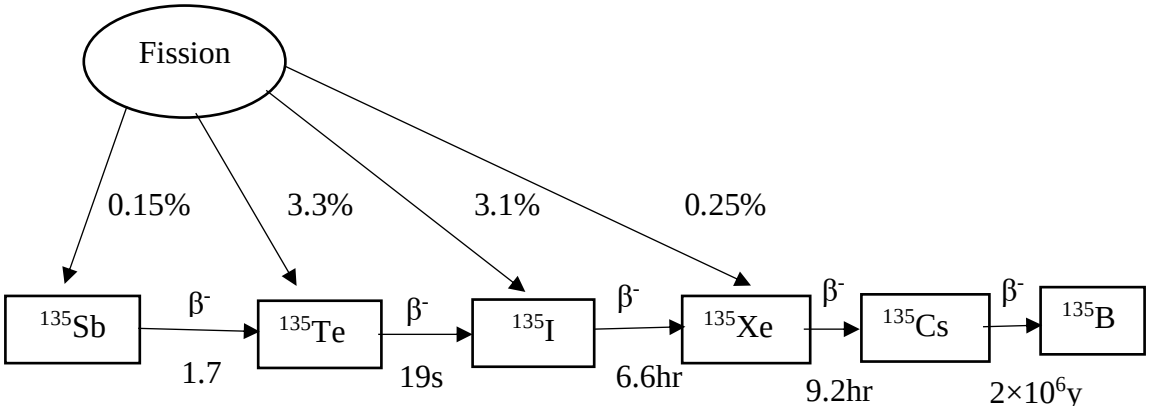

Figure 2: Production scheme of Xe-135 in nuclear fission

To study the dynamics of xenon-induced reactor power oscillations, let us consider a nuclear reactor with limited neutron flux coupled regions (Region 1 and Region 2), initially in steady state with the neutron flux and xenon concentrations are equal in both regions as shown in Figure 4 below. An initiating event of neutron reactivity change, such as the movement of control rod in Region 1, causes a decrease in the thermal neutron flux (ϕ) in Region 1. Region 1 experiences an immediate increase in Xe-135 (N_{Xe}) from decay of I-135 and a simultaneous decrease in the production of I-135 (N_I). Hence, the removal of Xe-135 through neutron capture will decrease while the

production of Xe-135 (from I-135 decay) remains at the previous equilibrium level. The net result is an increase in Xe-135 concentration (from I-135 decay) further decreasing the flux in Region 1. Again, this increased Xe-135 stays until its production (from iodine-135 decay) decreases to match with the decreased thermal flux, after which thermal flux levels will increase due to decreased removal of neutrons by Xe-135 capture. Increasing the flux by removal of control rod in the Region 2 increases the flux corresponding to the decrease of thermal neutron flux in Region 1.

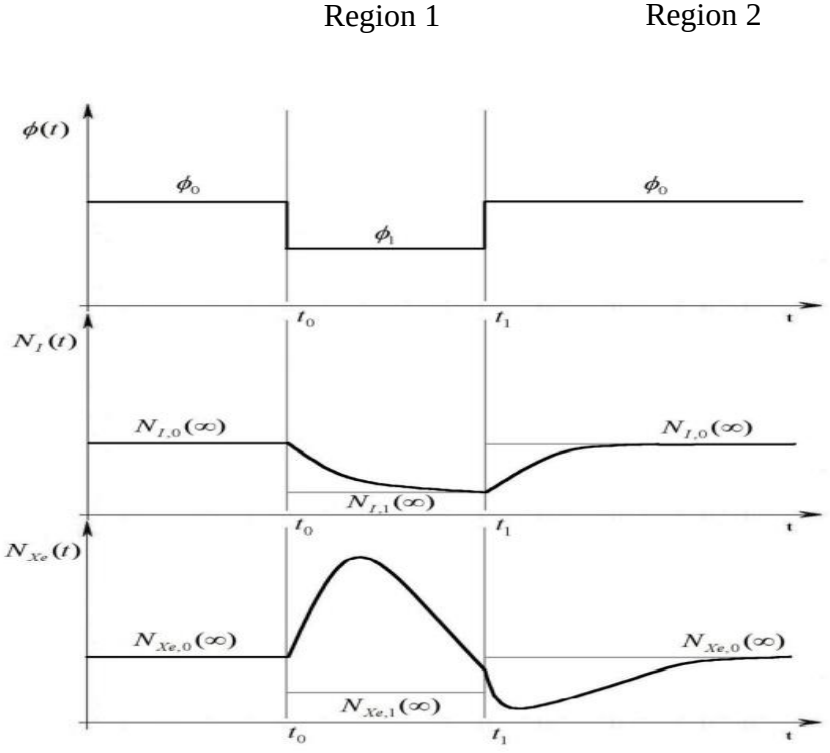

Figure 3: Time dependence of ^{135}Xe concentration following power-level changes

This imbalance will reverse as soon as an increased production of Xe-135 from I-135 starts in Region 2 compared to Region 1 resulting in the beginning of a Xe-135

oscillation. Depending on the design of the reactor core, these oscillations may be self-stabilizing and eventually dampen out, or they may continue to grow and threaten reactor operation. The bounding time scale for xenon dynamics is determined by the half-lives of I-135 and Xe-135 at 6.58 hours and 9.14 hours, respectively. Thus, typical oscillation periods are on the order of one day giving ample opportunity for xenon-induced power oscillations in commercial reactors to be controlled [18]

2.5.1 Axial Xenon Oscillation

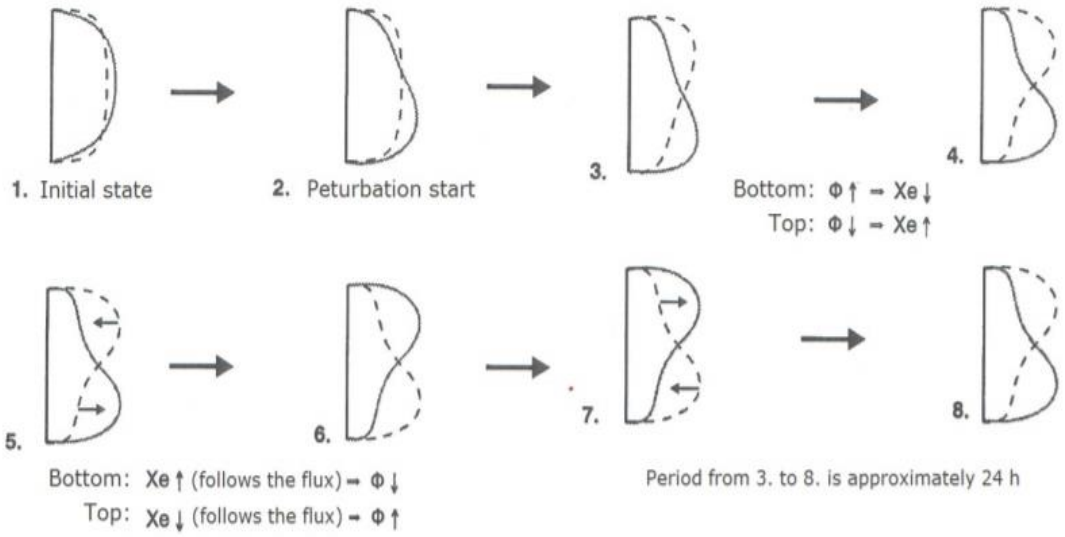

Figure 4: Axial xenon oscillation with axial profiles of nuclear reactor neutron flux (ϕ) and xenon concentration

Reprinted from B. Zajec, "Xenon Oscillations," University of Ljubljana, 2017 [17]

Oscillation is induced with control rod withdrawal, which leads to local increase of neutron flux and Xe-135 burnup at the bottom (steps 2 and 3). With increased flux at the bottom, increased I-135 production starts. Iodine then decays back to xenon with some delay, causing xenon concentrations to rise at the bottom and decline at the top (step 5). When profiles eventually reverse, process repeats with the opposite phase (step 7), causing xenon concentrations to slowly follow the flux profile and thus leading to initial perturbation. Thus, the neutron reactivity change in one region of the core will result in a decreased thermal neutron flux and a higher Xe-135 concentration while the other region will have a higher thermal neutron flux and lower Xe-135 concentration.

As described, processes rely primarily on iodine decay, period of xenon oscillations is in the order of magnitude of I-135 half life. The nature and stability of oscillations depend heavily on initial perturbation, reactor design and its operating conditions.

2.6 Simulation Approach

The desired neutronics analysis is performed to determine the threat posed to a typical *i*PWR-type SMR by potential xenon-induced power oscillation. The simulation approach is chosen to sufficiently account for the fundamental phenomena for the rate of change of xenon-135 within the reactor core and the spatial xenon-135 concentration in the core.

To do so, solving coupled multi-physics equations for neutron transport, fuel depletion, heat conduction in the fuel, convective heat transfer, and fluid flow within the

coolant channels with initial conditions, boundary conditions, and equations of state are essential.

This high level of complexity is needed in a single computational code that can sufficiently handle the above-mentioned physics intrinsically and the existence of state-of-the-art "single" physics codes has resulted in a common simulation approach, whereby an external routine is used to couple existing codes that handle one or two of the required physics. In this research this is achieved using the MCNP neutronics code with coupled thermal hydraulics. The MCNP code has been employed as the neutronics and fuel transmutation solver in many such routines. [19]

CHAPTER III

METHODOLOGY

In order to perform the desired neutronics and thermal hydraulics analyses for determining the threat posed to an (*i*PWR) SMR from xenon-induced power oscillations, the chosen computational approach should be able to simulate the rate of change of Xe-135 spatially and temporally within a three-dimensional model of the reactor core. Computational approach should be able to solve coupled multi-physics equations for neutron transport, fuel depletion and transmutation equations, thermal heat conduction within the fuel with fission and radiative capture source terms, convective heat transfer, and fluid flow within the coolant channels with the appropriate initial conditions, boundary conditions, and equations of state. [15]

The existence of the state-of-the-art "single" physics codes has resulted in a common simulation approach whereby an external routine is used to couple existing codes that handle one or two of the required physics phenomena. This is achieved using the Monte Carlo Radiation Transport Code, MCNP (neutronics and fuel transmutation code) by coupling it with an external thermal hydraulics algorithm.

3.1 Coupling Scheme

The multi-physics coupling computational methodology developed as part of this research involves simulating a generic SMR core model using the MCNP code coupled to a semi-analytic thermal hydraulics assessment algorithm.

1. The first step of the methodology is to determine spatial temperature distribution in the reactor core for a steady state condition with a given thermal power using MCNP code.

2. The results from this initial simulation is used to determine the temperature distributions of fuel, cladding, and coolant as well as the density distribution of coolant for the first small time-step of fuel depletion calculation, again using MCNP code.

3. The changed material compositions are extracted from the MCNP fuel depletion simulation output using Python script.

4. The volumetric fission heat generation rates for each axial fuel segment is evaluated using F7 tally (fission energy deposition) feature of MCNP.

5. These in conjunction with the inlet coolant temperature and pressure are used to calculate axial fuel and coolant temperature distributions using a semi-analytical approach. Coolant properties such as density for each axial coolant segment are determined as a function of temperature and pressure using the International Association for the Properties of Water and Steam (IAPWS) correlations.

6. Once the fuel temperature is determined, temperature dependent neutron reaction cross sections are generated using the weighted fraction calculation. [7]

7. These updated parameters are used in the updated MCNP input file for the fuel depletion simulation.

8. The above steps are repeated until each time step of the fuel depletion calculation is converged. The change in reactivity in two consecutive convergence steps with the

change in water density and temperature dependent weighted fractions of fuel ($\Delta\rho \leq$ 10mK) is less than or equal to 10 milli K is the convergence criteria.

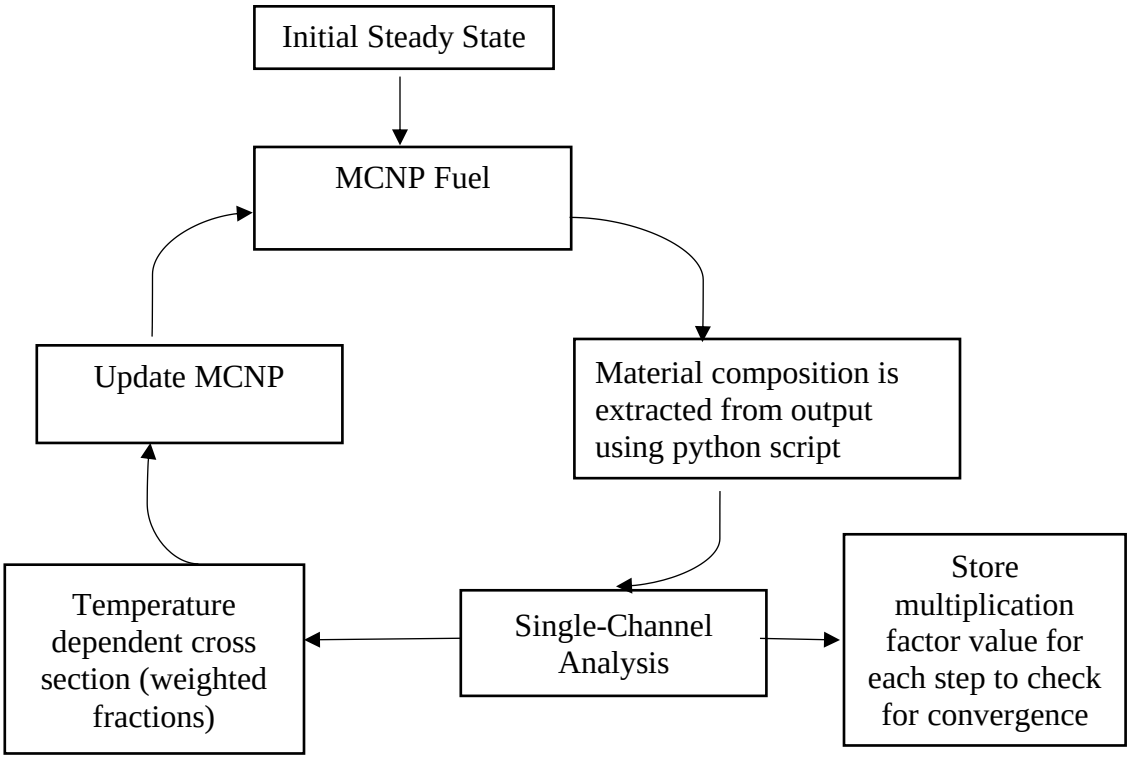

Figure 5: A system level flowchart of the developed multi-physics coupling routine

To observe the xenon oscillatory behavior, if any, in the reactor due to transients, multi-physics methodology is performed. This was performed by removing the control rod, partially, which in turn perturbs the neutron flux in a localized region of the core, initiating a xenon-oscillation in the reactor core. The perturbed system is evaluated using MCNP. The MCNP output file is parsed and material compositions including spatially dependent Xe-135 mass is extracted and plotted vs time to study the behavior of Xe-135 oscillations produced in the SMR core, key objectives being the estimation of the period

of the oscillation and how fast it disappears. The control rod was removed in only one specific assembly since, it is equivalent to 8 assemblies due to reactor core geometry.

3.1 Single channel analysis for thermal analysis

The Single Channel Analysis (SCA) tool used for thermal hydraulics analysis for this research is developed in Python. Analytical models and equations to determine axial fuel and coolant temperature distributions within each assembly in the reactor core are used in Python. Single isolated vertical flow fuel assembly channel is chosen for the SCA focusing the thermal hydraulics and thermodynamic analysis. In the previous research, solutions for the radial and axial fuel element temperature distributions were derived and are reproduced here for convenience. In the axial direction, the fuel, clad, and coolant temperature distributions are determined by using the core power distribution determined from the MCNP simulations. By applying Fourier's Law of Heat Conduction, in the heat equation, the linear heat generation rate is determined. For an analytical solution to be found, certain assumptions must be made. These include assuming steady-state heat transfer, one-dimensional thermal conduction, constant and evenly distributed fission heat source and constant material properties. The solutions for the temperature distributions in the fuel, gap, and clad in the radial direction is derived as:

$$T_F(r) = T_{max} - \frac{q_F'''}{4\,k_F} r^2; 0 \le r \le r_F \quad \text{..... (1)}$$

$$T_G(r) = T_{Cl} + \frac{q_F'''}{2\,k_G}\, ln\,(\frac{r_C}{r}); \quad r_F \le r \le r_{Cl} \quad \text{.....(2)}$$

$$T_C(r) = T_{Cl} + \frac{T_{Cl} - T_{CO}}{ln\,(\frac{r_{CO}}{r_{Cl}})}\, ln\,(\frac{r_{Cl}}{r}); \quad r_{Cl} \le r \le r_{CO} \quad \text{.....(3)}$$

Where, T_f = the temperature distributions in the fuel, T_g= Temperature distribution in the gap, T_C= Temperature distribution in the clad, T_{max} = Temperature at the center of the fuel, T_{Cl} = Temperature at the inner surface of the clad, T_{CO} = Temperature at the outer surface of the clad, R_f = Radii of the fuel region, R_{Ci} = Radii of the inner surface of the clad, R_{CO} = Radii at the outer surface of the clad.

Using Newton's law of cooling in conjunction with a known bulk coolant temperature, the solution for temperature at the outer surface of the clad is found [20]. By summation of the temperature changes over each region of the fuel element, the maximum centerline temperature is

$$T_{max} = T_{CO} + \frac{q'}{2\pi f_F}[\frac{r_F}{2k_F} + \frac{r_{Cl}-r_F}{k_G} + \frac{r_{CO}-r_{Cl}}{k_C} \quad \text{(4)}$$

In the axial direction, from nuclear reactor theory, the neutron flux shape for a bare cylindrical reactor with extrapolated height is a cosine function [16]. The heat conduction equation is solved analytically for each segment in the axial direction under the assumptions as the radial case:

$$T_b(z) = T_{in} + \frac{q'_{max}}{\omega C_P}(\frac{\hat{H}}{\pi})[\sin(\frac{\pi}{\hat{H}}z) + sin(\frac{\pi H}{2\hat{H}})] \quad \text{(5)}$$

$$T_{CO}(z) = T_{in} + q'_{max}[\frac{\hat{H}}{\pi\omega C_P}\{sin(\frac{\pi}{\hat{H}}z) + \sin(\frac{\pi H}{2\hat{H}})\} + \frac{1}{2\pi h r_{CO}}\cos(\frac{\pi}{\hat{H}}z)] \quad \text{(6)}$$

$$T_{CI}(z) = T_{CO}(z) + \frac{q'_{max}}{2\pi k_C} \times ln(\frac{r_{CO}}{r_f})\cos(\frac{\pi}{\hat{H}}z) \quad \text{(7)}$$

$$T_F(z) = T_{in} + q'_{max}[\frac{\hat{H}}{\pi\omega C_P}\{\sin(\frac{\pi}{\hat{H}}z) + \sin(\frac{\pi H}{2}) \quad \text{(8)}$$

The axial temperature profile of the fuel, cladding inner, cladding outer and coolant in the reactor core is represented in Figure 7 below.

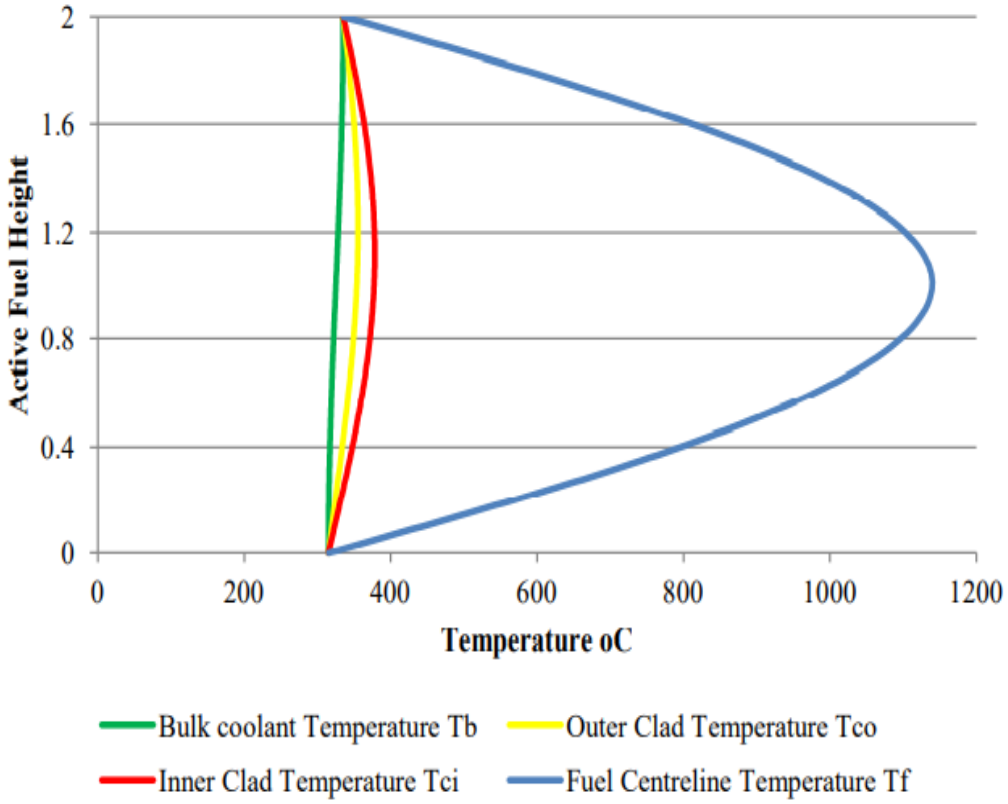

Figure 6: Axial Temperature variation of fuel, cladding and coolant with respect to fuel height [16]

Reprinted from J. R. Lamarsh, Introduction to nuclear reactor theory, Addison, 1972 [16]

3.2 Description of tools

The MCNP6 code was used to perform the reactor core physics calculations. The thermal hydraulics single channel analysis of the fuel channel is done analytically. This is done using Microsoft EXCEL and Python code developed.

3.2.1 MCNP

The Monte Carlo method is a numerical technique that produces approximate solutions to problems. The cornerstone of this method is the repeated random sampling

of a probability distribution similar in nature to the throwing of dice at a gambling table in Monte Carlo and hence its name [1]. By choosing appropriate probability distributions to sample, that are characteristic of the problem being solved, a numerical solution can be obtained. In the case of neutron transport, it is finding the solution of the Boltzmann Radiation Transport Equation [1]. The Monte Carlo method simulates the transport of individual particles within the problem phase space, determines specific details of each particle transport within the phase space and approximates the overall solution as the averaged particle behavior after simulating many particles.

Unlike deterministic methods way of solving the Boltzmann Transport Equation, which generally gives a solution over the entire phase space for all predetermined quantities such as o=flux, current etc., the Monte Carlo method typically solves for user specified quantities in user defined portions of the problem phase space. As mentioned, the Monte Carlo method is determined by random sampling of appropriate probability distributions. In order to do so, many Monte Carlo codes, including MCNP, use Linear Congruential Generator algorithms to produce an essentially inexhaustible list of random numbers [1].

The events that comprise a particle history are determined by probabilities such as nuclear transport data governing the transport of the particle type through the materials specified in the problem. As such, random numbers are used to determine the location, distance, and direction of the particle interaction, the nuclide with which it interacts and the type of interaction and the resulting changes to the nuclide and particle because of the interaction. This stochastic process is repeated many times to achieve convergence

to the solution of the problem being solved via the Monte Carlo simulation. Complex three-dimensional problem geometries are solved using Monte Carlo methods where the nodal discretization of the problem phase-space prove to be a hindrance to the application of deterministic methods. Codes such as MCNP support the desire for high fidelity modeling of the reactor core neutronics needed for this research.

3.2.2 CINDER 90 for fuel depletion

The CINDER90 module in the MCNP6 code uses Markov chains to solve the set of coupled differential equations that constitute the nuclide transmutation equations [21]. CINDER90 is the current version of the CINDER code (also developed at Los Alamos National Laboratory) and features decay and interaction probability data for 3456 nuclides including 30 fission yield sets, and yield data for 1325 fission-products [21] [22] [23]. The differential equations solved in CINDER90 are a simplified form of the Bateman equations as shown below:

$$\frac{dN_m}{dt} = -N_m(t)\beta_m + \sum_{k\neq m} N_k(t)\gamma_{k\to m} + \bar{y}_m \quad \text{(9)}$$

$$\beta_m = \lambda_m + \sum_r \int \sigma_{m,r}(E)\varphi(r,E,t)dE \quad \text{(10)}$$

$$\gamma_{k\to m} = \sum_{m\neq k} L_{km}\lambda_k + \sum_{m\neq k}\sum_r \int Y_{km,r}(E)\sigma_{k,r}(E)\varphi(r,E,t)dE \quad \text{(11)}$$

where $\frac{dNm}{dt}$ is the rate of change of the nuclide density of m, $-N_m(t)\beta_m$ is the destruction rate of nuclide m, $\sum_{k\neq m} N_k(t)\gamma_{k\to m}$ is the production rate of m summed over all other nuclides, $\bar{y}_m$ is the production rate of m from an external source, λ_m is the destruction rate of m by radioactive decay, $\sum_r \int \sigma m, r\,(E)\varphi(r,E,t)dE$ is the destruction

of m by transmutation into all other nuclides summed over all transmutation reactions, $\sum_{m\neq k} L_{km}$ is the production rate of m from the decay of all other nuclide and is the summation of the production rate of m by transmutation of all other nuclides summed over all transmutation reactions.

Based on the given criteria, a set of nuclear data is used strategically to determine which production/destruction chains to include in the simulation. Markovian chains are then used to solve for differential equations to determine the concentration of a nuclide that have production/destruction mechanisms for the nuclide of interest linearizing the chosen set of equations. The CINDER90 code must be coupled with a steady-state reaction rate calculator to capture the temporal evolution of reaction rates within a system such as a reactor core. MCNP provides this capability, supplying CINDER90 with updated reaction rates at each user determined time interval.

Thus, in a MCNP6 depletion simulation, an initial material composition is provided to MCNP via the user input deck. MCNP is used to calculate material specific neutron fluxes and reaction rates using a standard five-group structure [7]. These neutron flux and reaction rate tallies together produce an effective one-group neutron flux and reaction rate by which an effective one-group cross section is determined and passed to CINDER90. The CINDER90 module then uses this material specific one-group cross section along with its extensive nuclide data set to evaluate a fuel depletion calculation to obtain new nuclide densities for each material at the end of the user specified time interval. These material densities are returned to MCNP6 for the transport simulation of

the next time step to be performed. This process is repeated until all time steps specified by the user in the input deck have been completed.

CHAPTER IV

REACTOR DESIGN

The SMR design selected for the computational study is a light water cooled and light water moderated pressurized reactor of the integral PWR (*i*PWR) type with a rated thermal power output of 530 MWth. Height to diameter ratio for a typical PWR is 1.4 whereas for the current SMR reactor design, H/D ratio is 1.23.

4.1. Existing PWR Assembly Parameters

To facilitate licensing and promote safety through over half a century of operating experience, as mentioned in the design objectives, there are a host of technology transfers from existing large PWRs to this SMR design. With respect to materials and dimensions except for the active fuel length, the SMR fuel assemblies are to be exactly the same as the typical existing large PWR. As such a typical 17x17 fuel assembly configuration is chosen. Figure 8 shows the geometry of a single fuel cell modeled in MCNP. The fuel assembly parameters used in the model were kept the same as the existing large PWR and are presented in Table 1 [16].

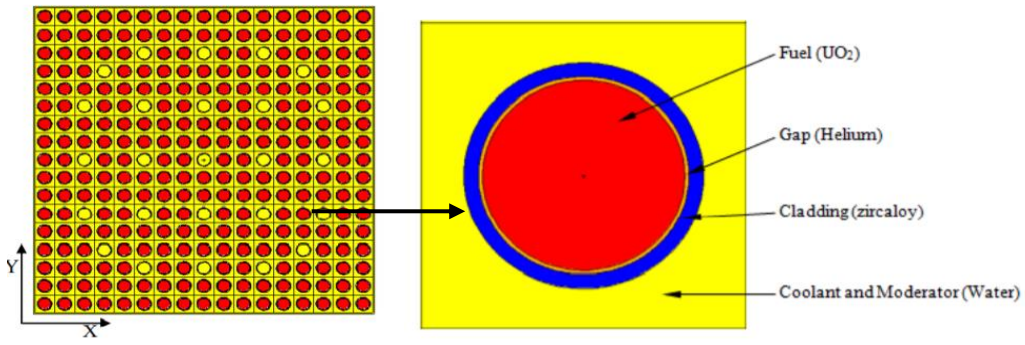

Figure 7: Radial PWR Fuel Pin Geometry of the SMR design

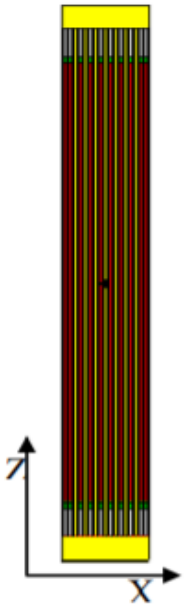

Figure 8: Axial cross section of a single fuel assembly

4.2 Fuel Enrichment

The fuel material is low enriched uranium (LEU) uranium dioxide (UO_2). The PWR cores typically will have fuel assemblies with a range of uranium enrichment levels. For use in commercial reactors, LEU is enriched to between 3 and 5% ^{235}U. The fuel rod consists of low enriched UO_2 pellets with a helium gap surrounding the fuel pellet and the zirconium alloy cladding. The active fuel length is 240 cm. The fuel enrichments are varied between 4.4% and 4.95% for flattening neutron flux in the reactor core.

Figure 9 (a): Axial cross section of the SMR Model

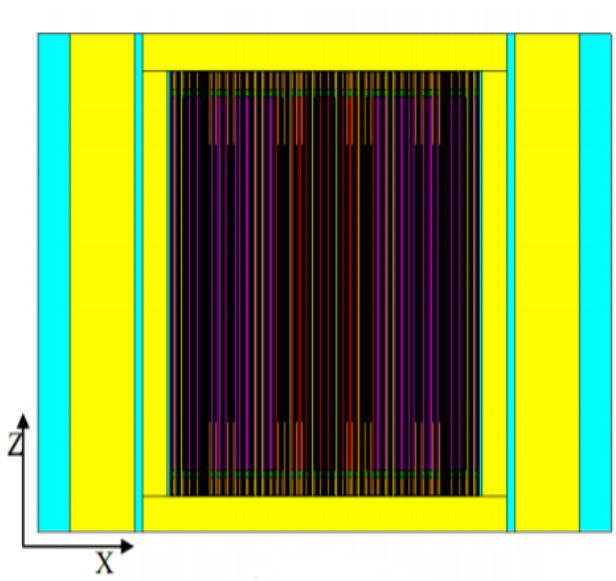

Figure 9 (b): Radial Cross Section of the SMR core Model geometry

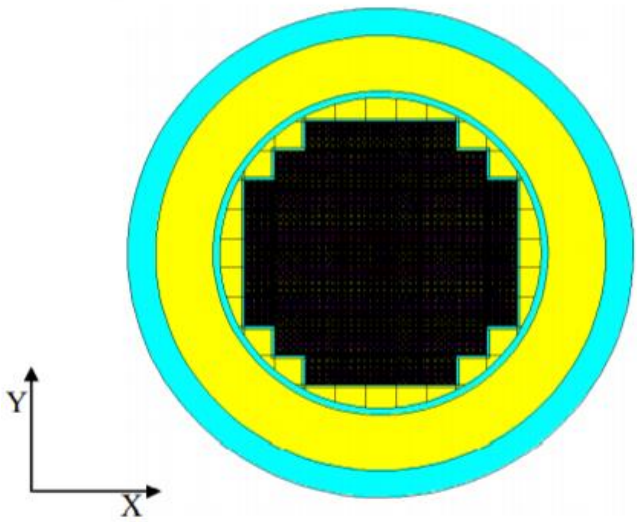

4.3 Reactivity Control

The initial core loading would have Burnable Absorber Rods (BARs) made of B_4C to aid with flattening the neutron flux, hence core power profiles, to reduce power peaking and also to achieve uniform fuel burnup [6]. PWRs also operate using fuel integral BARs but is not done in this SMR core selected for the study. The absorber material in the SMR core is natural boron carbide (B_4C) with 19.9% ^{10}B. [6]In addition to BARs and control rods, existing large PWRs use soluble boron in the coolant and moderator as a means of controlling the reactor core . In the SMR, the reactivity control would be entirely through the movement of control rods. There is no soluble boron in the light water coolant/moderator of the SMR being modelled

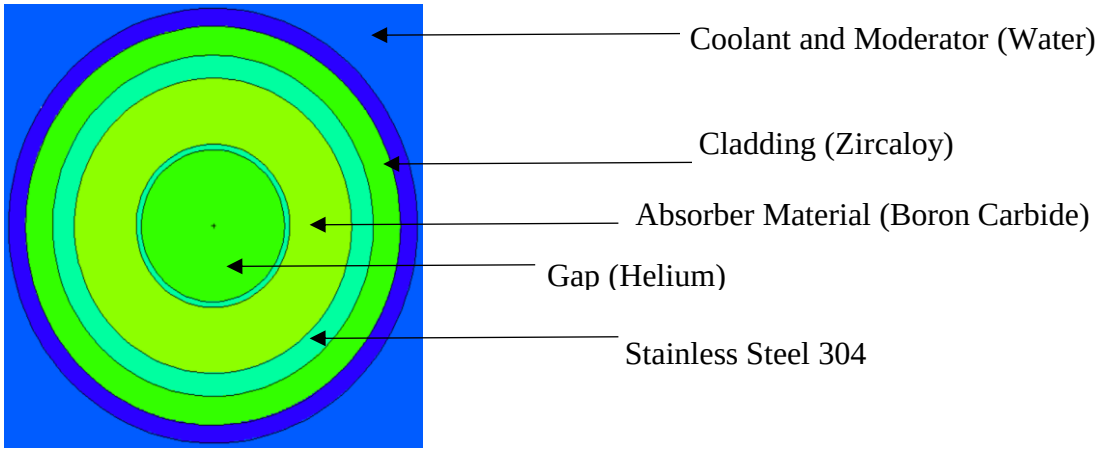

Figure 10: Radial Cross section of the burnable absorber rod (BAR)

4.4 SMR Core model using MCNP

The developed simulation methodology must exhibit sufficient fidelity with respect to the determination of the spatial shape of the neutron flux within the *i*PWR SMR core. Using the radial symmetry of the optimized core model, a one-eighth core model was developed reducing computational time of the depletion simulations. This model featured thirteen assembly locations as shown in Figure 12. Each fuel assembly was divided axially into eight segments. Each axial segment was given its own material definition in MCNP6 input allowing for axially dependent neutron flux and isotopic concentrations within the fuel to be tracked in the fuel depletion simulations.

Similarly, coolant channels within the assemblies were divided into axial segments; one per axial fuel segment. The SCA tool was also updated to allow coolant temperatures and densities for each of these volumes to be calculated. Core average coolant temperatures were calculated and assigned to the coolant volumes between assemblies.

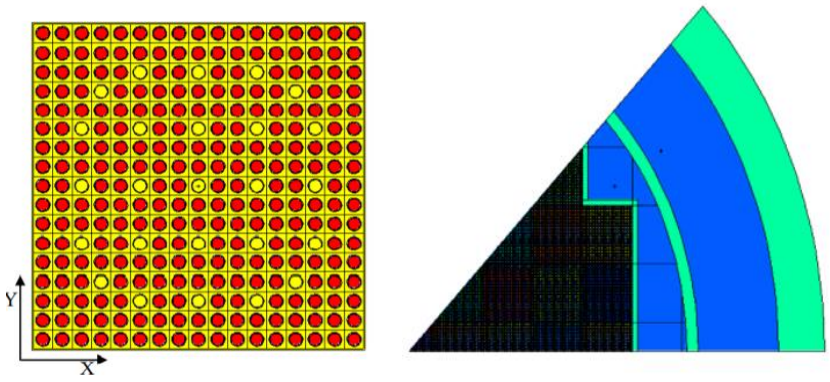

Figure 11: Radial Cross Section of SMR Model

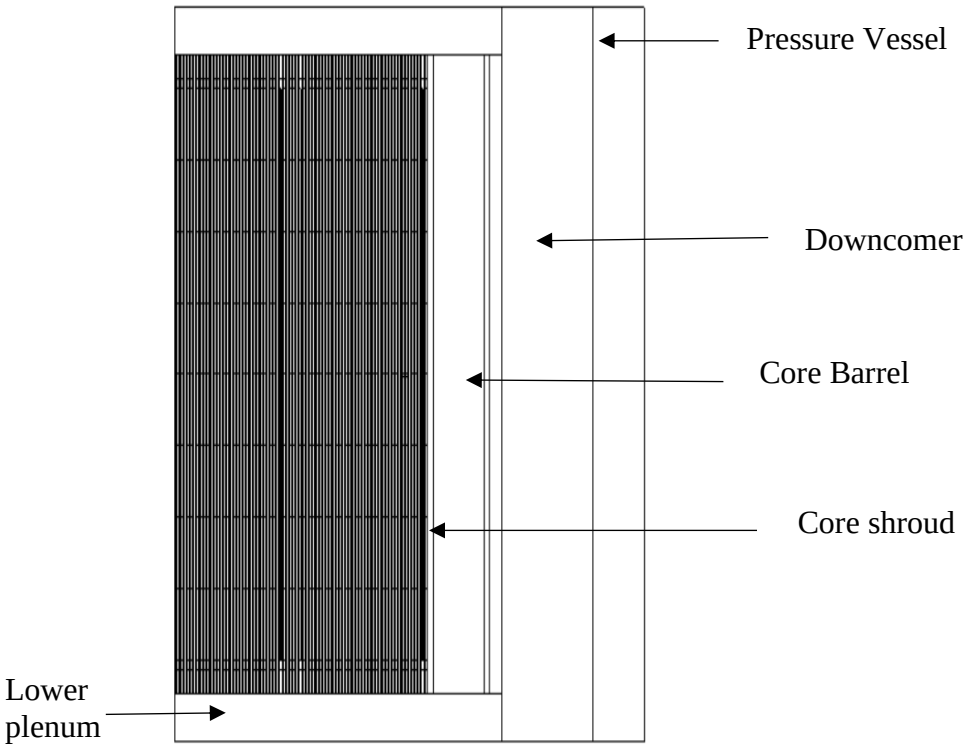

Figure 12: Axial Cross Section of SMR Model (Fuel Regions Visible)

Table 1: PWR Fuel Assembly Details Used for the SMR Assembly

Fuel rod parameter	**Value**
Fuel Material	UO_2
Fuel Enrichment	Various (all<5%)
Fuel pellet diameter (cm)	0.784352
Gap material	Helium
Gap outer diameter (cm)	0.815848
Clad material	Zircaloy- 4
Clad outer diameter (cm)	0.930148

Table 1 Continued

Fuel rod parameter	Value
Fuel lattice pitch (cm)	1.25984
Assembly size	17×17
Fuel rods per assembly	264
Guide tubes	25

4.5 Burnable Absorber Rod

The developed SMR core model reveal a design with similar characteristics to existing large commercial PWRs. The burnable absorber rod material and configuration is assessed to provide initial insight to the differences, if any, between PWR and SMR reactivity control in the absence of soluble boron in the coolant.

4.5.1 Methods for Excess Reactivity Control

Currently, there are three main methods employed in PWRs to achieve excess reactivity control [15]. The first method involves the insertion of strong neutron absorbing material into the reactor core in the shape of control rods. The strong neutron absorbing material in the control rods reduce the number of neutrons available to initiate the fission reaction. The amount of control exerted by the control rods is a function of length of the rod(s) inserted into the core. The insertion length is controlled by the operator of the reactor and provides an active mechanism for controlling core power. The second method is to mix the strong neutron absorbing materials into the fuel material itself. In this configuration, the amount of absorber introduced to the core must be

determined at the beginning of core life and is fixed once the core has been loaded. As the strong absorbing material captures neutrons, it will be depleted over time. As such these burnable absorbers are used primarily to suppress the initial excess reactivity in the core at beginning of core life. The third method is to introduce the strong absorbing material in a soluble form dissolved into the coolant. PWRs are thermal reactors, meaning, most of the fissions within the nuclear chain reaction are caused by neutrons of thermal energy. However, initially all neutrons produced in nuclear fission have fast energies and need to be slowed down (or thermalized) in order to continue the nuclear fission chain reaction. The fast neutrons produced in the fuel are thermalized in the coolant which also serves as a moderator. By adding strong absorbing material to the coolant, a fraction of the thermalized neutrons can be removed before returning to the fuel to cause fission thus controlling the fission chain reaction. This method allows for active control of excess core reactivity since the concentration of strong absorbing material in the coolant can be controlled by a Chemical Volume Control System which can add or remove the absorber material as needed as the fuel depletion progresses.

4.5.2 Implications of a Boron Free Coolant in SMR Operations

In PWRs, the soluble absorber material of choice is typically soluble boron in the form of boric acid. A major advantage of using soluble boron is that unlike control rods and burnable absorbers which provide localized neutron reactivity control, soluble boron can provide a more universal neutron reactivity control as the absorber material is efficiently distributed throughout the core by the coolant. Hence, eliminating soluble absorber material offers many advantages to the SMR operation. These include the

removal of all systems associated with the manipulation of the boron concentration in the coolant (pipes, pumps, and purification systems) and the elimination of the corrosive effects of boric acid within the coolant. Therefore, accident scenarios are eliminated, which are initiated by the movement of a volume of coolant that is void of boron or rich in boron through the core. This coolant volume can result in very localized, strong, positive, or negative reactivity insertions resulting in transients which could lead to reactor shutdown. In addition, avoiding boron in the coolant reduces the amount of undesired radioactive material production.

CHAPTER V

RESULTS AND DISCUSSION

Before assessing the threat posed to the reactor model by xenon-induced power oscillations, the developed methodology was applied to a typical depletion calculation to assess the effect of updating fuel material cross sections and coolant temperatures and densities at each fuel depletion time step. The results of this preliminary assessment are presented in Section 5.1.

5.1 Effective Neutron Multiplication Factor and Fuel Burnup

The change in effective neutron multiplication factor as function of time due to various aspects; reactivity decrease associated with the Doppler broadening of the uranium-238 radiative capture cross section, buildup of fission products, and fuel depletion are discussed in this section (Figure 14). The fuel material temperatures are implemented in the shape of updated material cross sections in all eight axial regions of the fuel with increased fuel temperatures compared to the basic model of the previous research. The increase in fission reaction rate in uranium-235 is compensated by increased resonance absorption of neutrons in uranium-238.

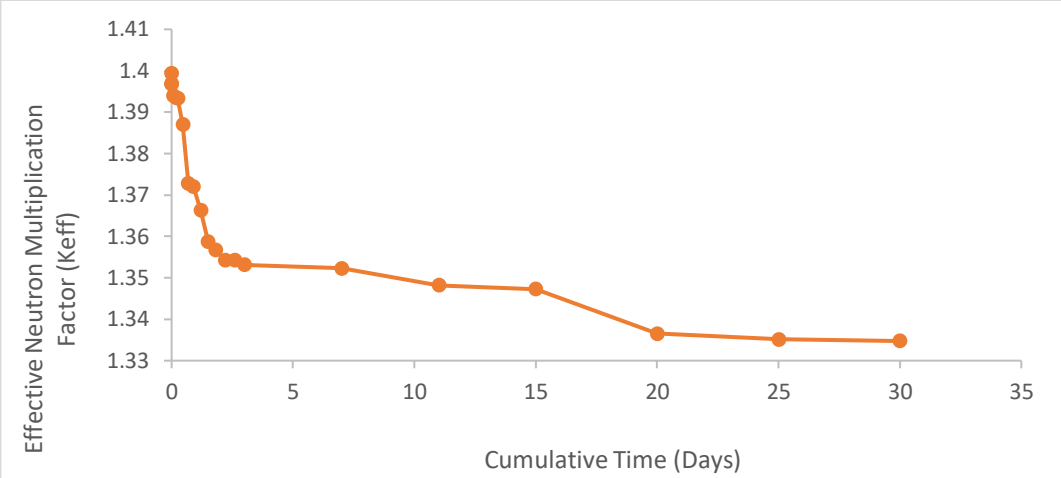

Figure 13: Plot of Effective multiplication factor vs time in days

Temperature variations cause changes in physical characteristics of the fuel material such as density, affecting the heat production rates through fission. The physical properties that are temperature dependent, other than the density of the fuel, include the material thermal conductivity which largely affects the rate at which heat is produced in the fuel and is dissipated through the gap and cladding to the coolant.

The increase in resonance absorption leads to a net decrease in fission rate and a decrease in the effective multiplication factor. The increased fuel temperatures are accompanied by increased coolant temperatures and decreased coolant region densities along the active fuel length. As the density decreases, the moderation offered by the coolant in the core also decreases resulting in a harder neutron spectrum and an accompanying decrease in effective neutron multiplication factor as expected in a reactor designed to operate in the thermal spectrum [16].

Fuel burn-up increases linearly with time as the amount of energy output from the core per unit time is constant. The first ten days of the simulation are executed in

time steps of 0.0833, 0.21667, 0.30, 0.4, 4 and 5 days to accurately simulate the buildup of short-lived fission products, specifically ^{135}Xe. This sequence was selected to allow xenon and other fission products to build up to their equilibrium levels. Figure 15 shows the xenon mass reaching saturation.

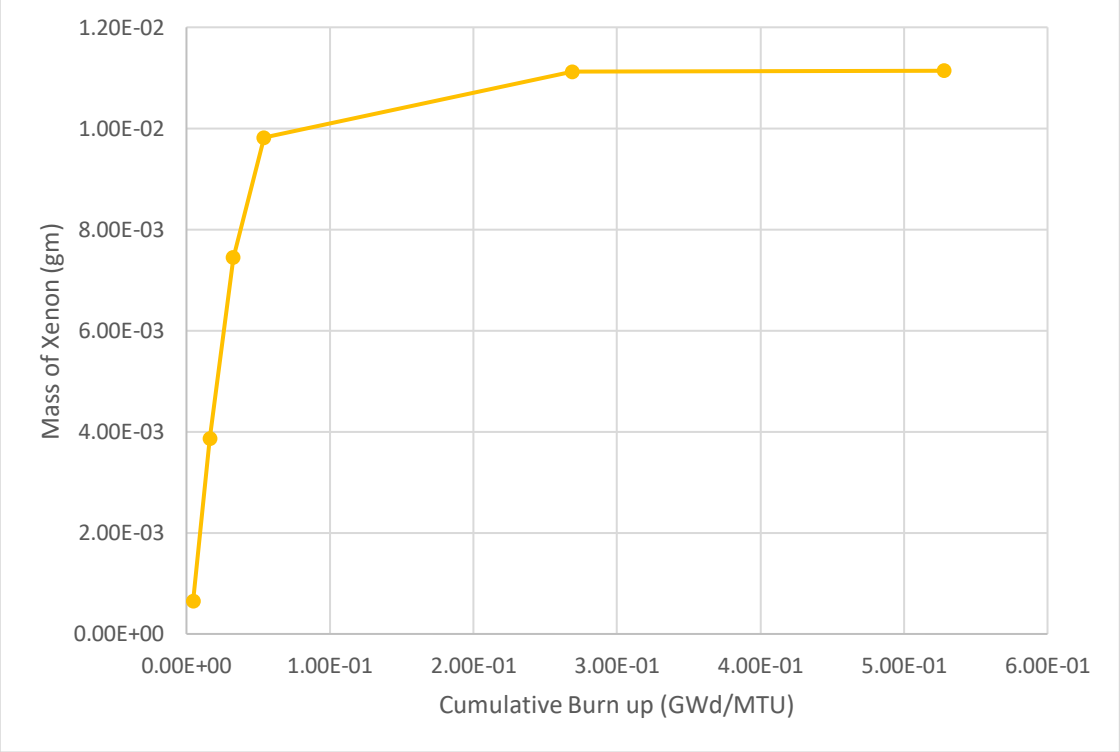

Figure 14: SMR ^{135}Xe Mass vs Burnup of the fuel

As mentioned previously, increased uniformity of the neutron flux distribution leads to decreased xenon stability. Hence, xenon production/destruction with power is an important topic of study. The evolution of the core-averaged axial volumetric heat generation rate is presented in Figure 16. The temperature profile in fuel, cladding, and coolant are shown in Figure 17. After equilibrium xenon concentrations are established

at ten days, the axial power profile is “bottom-peaked” due to increased moderation (reactivity) as colder more dense coolant enters the core from the lower plenum. The “bottom-peaked” nature of the power profile is more pronounced in the central assembly and less so the core average distribution is calculated. With further depletion, the power profile becomes increasingly uniform.

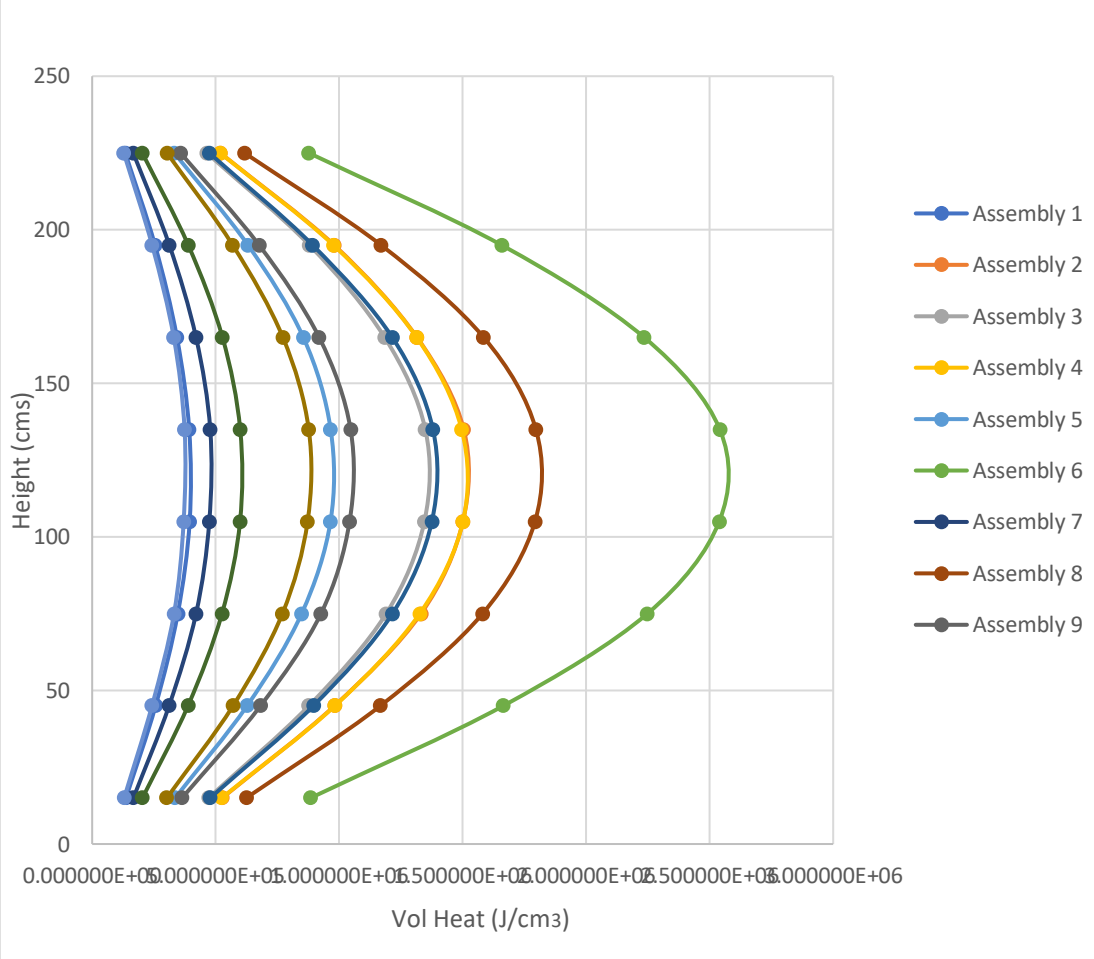

Figure15: Plot of Volumetric Heat generation rate with Height of the fuel at steady state

At steady state, the volumetric heat generation rate of the fuel in the reactor core represents a cosine function with respect to the height of the core. As the fuel in the reactor core is burned eventually in multiple time steps, the shape of the volumetric heat generation rate of the fuel depicts a bottom peaked curve which is represented in Figure 18 below. In Fig.20, the inlet temperature of the coolant which enters from the bottom of the core is 300 °C and the coolant exits the core at temperature around 330 °C. Hence lower coolant temperature is denser at the bottom and therefore, the neutrons are highly moderated by the denser coolant which is evident by the bottom peaked curve.

The bottom region of the core experiences increased fission due to the increased moderation, however over time, this increased fission leads to increased depletion of the fissile isotope content in the fuel. As this occurs, the net reactivity of the bottom region of the core decreases and the power produced. Some stochastic variation is observed at subsequent time steps as the MCNP code attempts to enforce a constant power condition. This behavior is typical of Monte Carlo radiation transport simulations [18].

As the axial power distribution and the fuel centerline axial temperature distribution are linked, the trends observed are evident in both cases. Figure 19 shows the evolution of the core-averaged fuel-centerline axial temperature distribution. As the axial volumetric heat generation rate becomes increasingly uniform with time, so too does the fuel-centerline axial temperature distribution. From the figure, peak fuel centerline temperatures are well within safe operating limits for LEU fueled light water reactors as set forth in the Code of Federal Regulations (10CFR50.46). [24] The core averaged bulk coolant axial temperature distribution is shown in Figure 20. As a result

of the initial “bottom-peaked” nature of the axial power distribution, the rate of heat addition to the bulk coolant is at a maximum in the bottom coolant segments. As the axial power distribution becomes increasingly uniform, so too does the rate of heat addition to the bulk coolant resulting in a more linear increase in bulk coolant temperature with time. The core averaged outlet temperature is approximately 323 °C with an initial inlet temperature set at 297 °C, which is typical of existing PWRs. With the reactor vessel pressurized to 14.1 MPa, the bulk coolant is firmly within the subcooled boiling heat transfer regime [25] desired for safe operation.

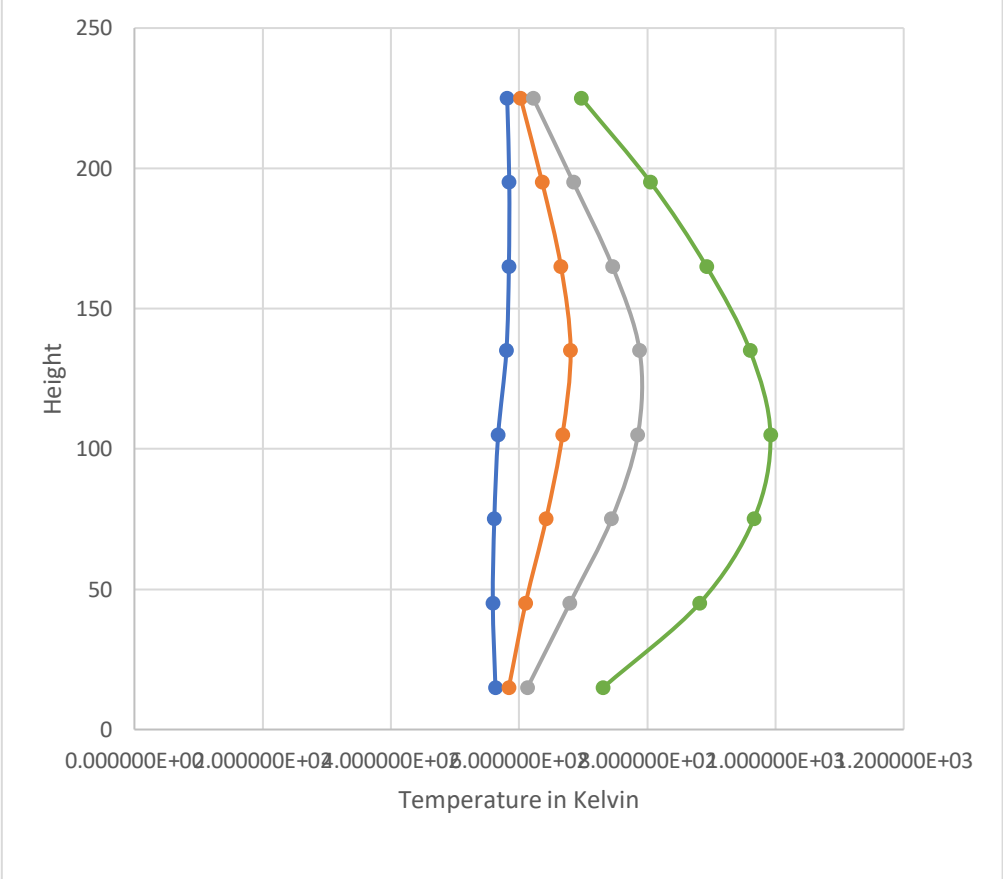

Figure 16: Temperature Profile of Fuel, Cladding inner and outer and Coolant in the core

As the coolant moves along the fuel element, it absorbs heat; as a result, its temperature continuously increases. However, the temperature does not increase axially at a constant rate since the heat is released from the fuel non-uniformly.

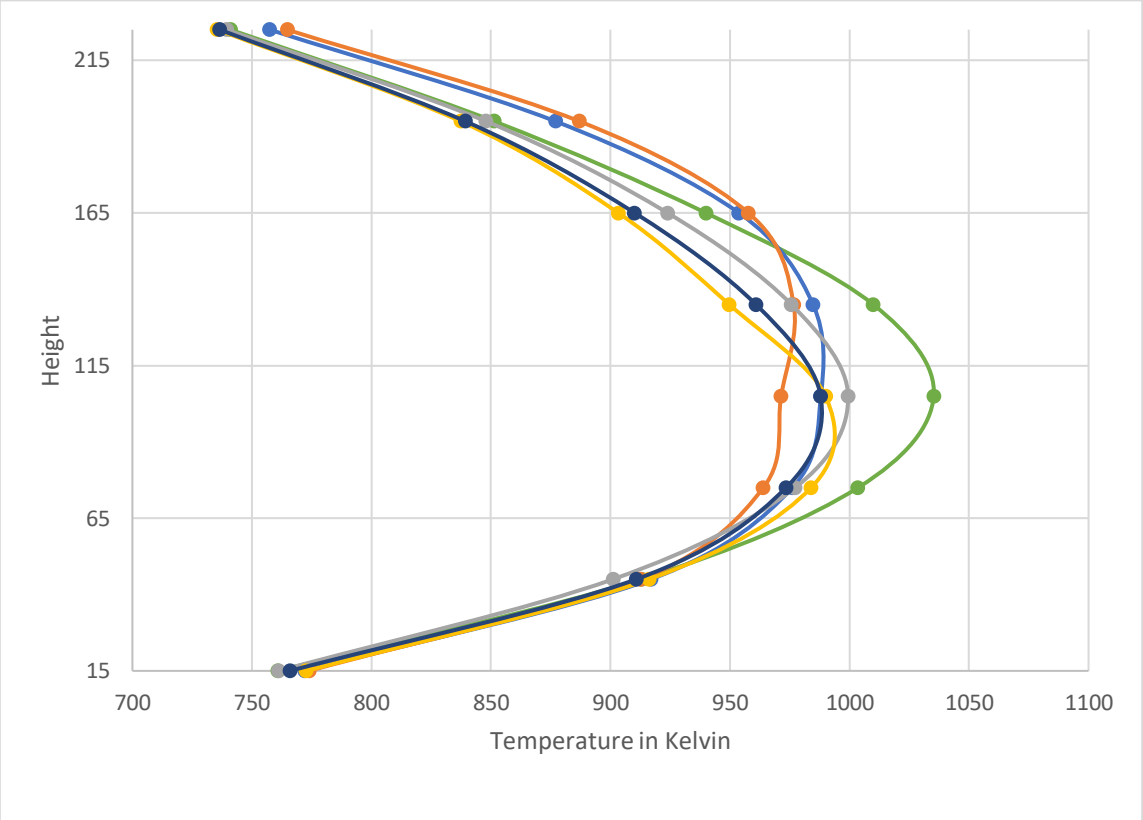

Figure17: Evolution of Axial temperature profile of fuel

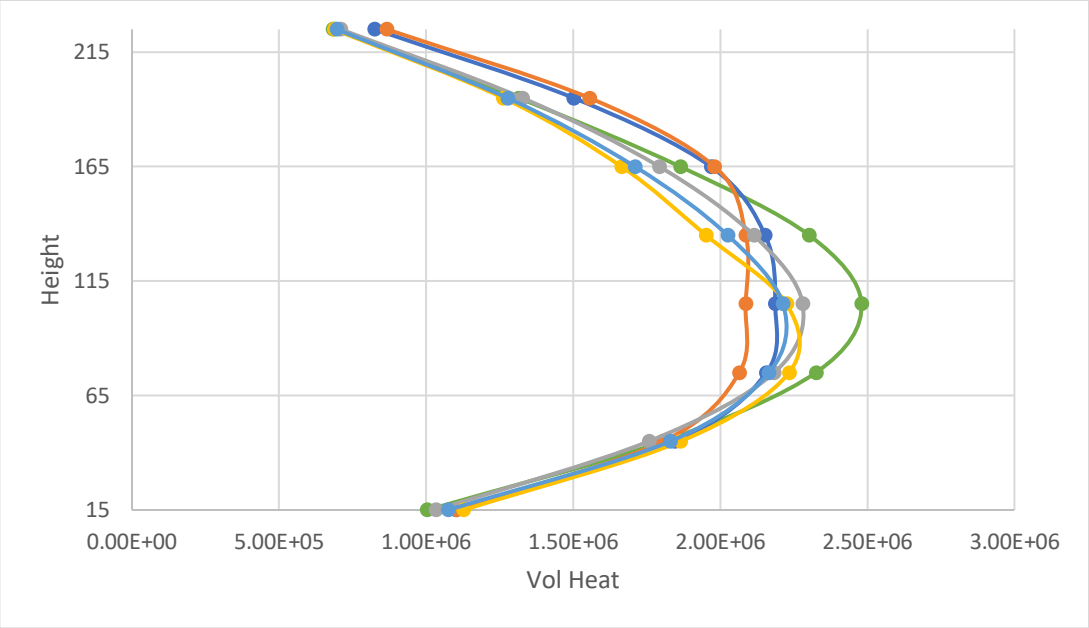

Figure 18: Evolution of Volumetric heat generation rate in the fuel with burnup

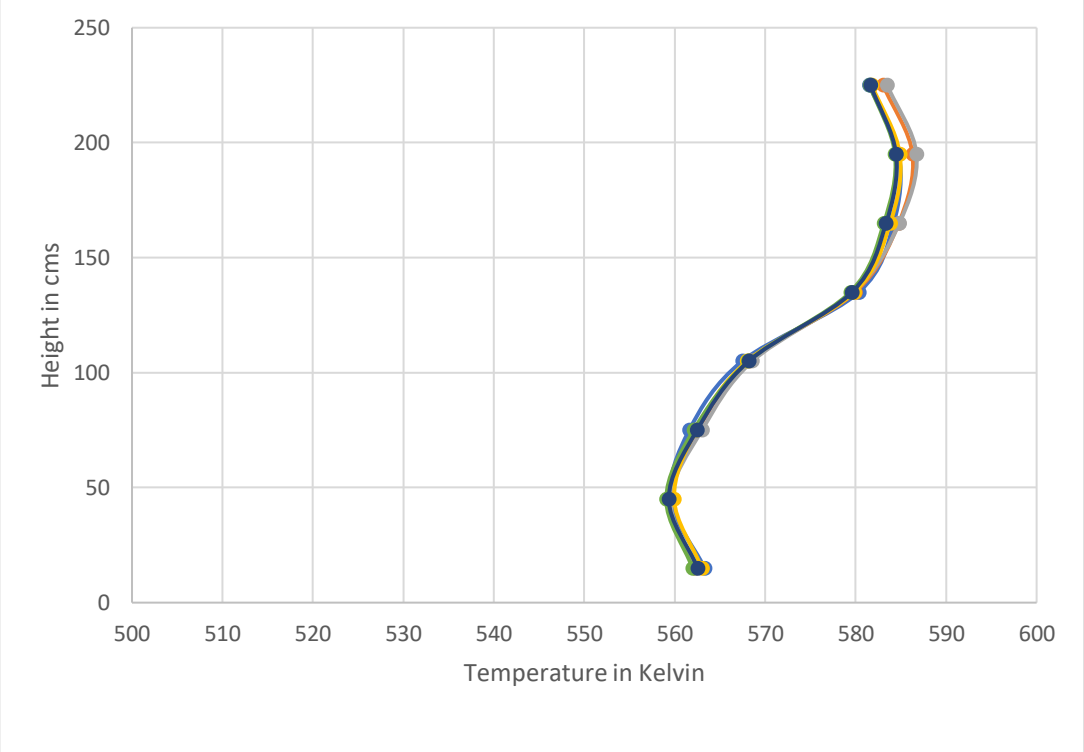

Figure 19: Evolution of Axial Bulk Coolant temperature in the SMR core model

Fuel Depletion Convergence

Initially the temperature distribution in the reactor core is evaluated for steady state with a given thermal power using MCNP code. The effective neutron multiplication factor, k_{eff} for the steady state was found to be 1.39932. F7 tally (fission energy deposition estimate) in MCNP is used for evaluating the heat generation rate in the 8 axial segments of the fuel. The evaluated volumetric heat generation rate is extracted to the MS excel sheet using Python script. The results from this initial simulation is used to determine the temperature distributions of fuel, cladding, and coolant as well as the density distribution of coolant. The temperature distribution of fuel, clad and coolant is evaluated using equations (5) to (8) for the steady state.

From the evaluated temperatures of the fuel, the weighted fractions of the ^{235}U and ^{238}Uin the fuel are calculated using equations 5 and 6. To approximate the cross sections for uranium nuclide in the fuel at temperature T, a weighted combination of the nuclide at lower temperature T_1 and higher temperature T_2 is used. The weighted combination is input as a MCNP material with volume fractions [7]. The fuel temperature cross section extensions are chosen based on the evaluated temperatures. The range of cross section extensions with their respective temperatures is depicted in Table 2.

$$W_2 = \frac{\sqrt{T}-\sqrt{T_1}}{\sqrt{T_2}-\sqrt{T_1}} \quad \text{(12)}$$

$$W_1 = 1 - W_2 \quad \text{(13)}$$

$$\sum\nolimits_i = \sum (T_i)$$

$$\sum (T) = W_1 . \sum\nolimits_1 + W_2 . \sum\nolimits_2$$

Where, W_1 = Weighted fraction of the nuclide at lower temperature and $W_2 =$ Weighted fraction of the nuclide at higher temperature.

Table 2: Temperature dependent fuel cross section extensions

Temperature in Kelvin	Cross Section Extensions
300	.70C
600	.71C
900	.72C
1200	.73C
2400	.74C

These in conjunction with the inlet coolant temperature and pressure are used to calculate axial fuel and coolant temperature distributions using a semi-analytical approach. Coolant properties such as density for each axial coolant segment are determined as a function of temperature and pressure using the International Association for the Properties of Water and Steam (IAPWS) correlations [26].

The above steps are repeated until each time step of the fuel depletion calculation is converged. The change in reactivity in two consecutive convergence steps with the change in water density and temperature dependent weighted fractions of fuel ($\Delta\rho \leq$ 10mK) is less than or equal to 10 milli K is the convergence criteria.

The change in reactivity $\Delta\rho$, is calculated as

$$\Delta\rho = \frac{K_{eff2} - K_{eff1}}{K_{eff1} \times K_{eff2}} \times 1000\, mK$$

The multiplication factor for the burn time steps 0.083, 0.21667, 0.3, 0.4, 4, 5 and their corresponding convergence steps are tabulated in Table 5.

Table 3: Effective Multiplication Factor for fuel depletion convergence

	Time Steps (days)	**Effective Multiplication Factor (K_{eff})**		**Change in Reactivity $\Delta\rho$ (mK)**
Steady State	0	K_{eff1}	1.39932	0.1025
		K_{eff2}	1.39696	
		K_{eff3}	1.39676	
Burn 1	0.083	K_{eff1}	1.39402	0.05665
		K_{eff2}	1.39350	
		K_{eff3}	1.39339	
Burn 2	0.21667	K_{eff1}	1.38705	0.41413
		K_{eff2}	1.37277	
		K_{eff3}	1.37199	
Burn 3	0.3	K_{eff1}	1.36636	1.03610
		K_{eff2}	1.35870	
		K_{eff3}	1.35679	

Table 3 continued

	Time Steps (days)	**Effective Multiplication Factor (K_{eff})**		**Change in Reactivity $\Delta\rho$ (mK)**
Burn 4	0.4	K_{eff2}	0.5566	0.5566
		K_{eff2}	1.35420	
		K_{eff3}	1.35318	
Burn 5	4	K_{eff1}	0.50097	0.50097
		K_{eff2}	1.34822	
		K_{eff3}	1.34731	
Burn 6	5	K_{eff1}	0.21884	0.21884
		K_{eff2}	1.33513	
		K_{eff3}	1.33474	

From the above table, it is proven that the change in reactivity $\Delta\boldsymbol{\rho}$ in milli K is less than 10 mK. Hence the fuel depletion calculation is converged ($\Delta\rho < 10$mK) at each time step. The volumetric heat generation rate convergence and the temperature convergence at time step 0.083 days is depicted in Figure 21 below.

Figure 20: Evolution of Fuel, cladding and coolant temperatures for fuel depletion convergence calculation

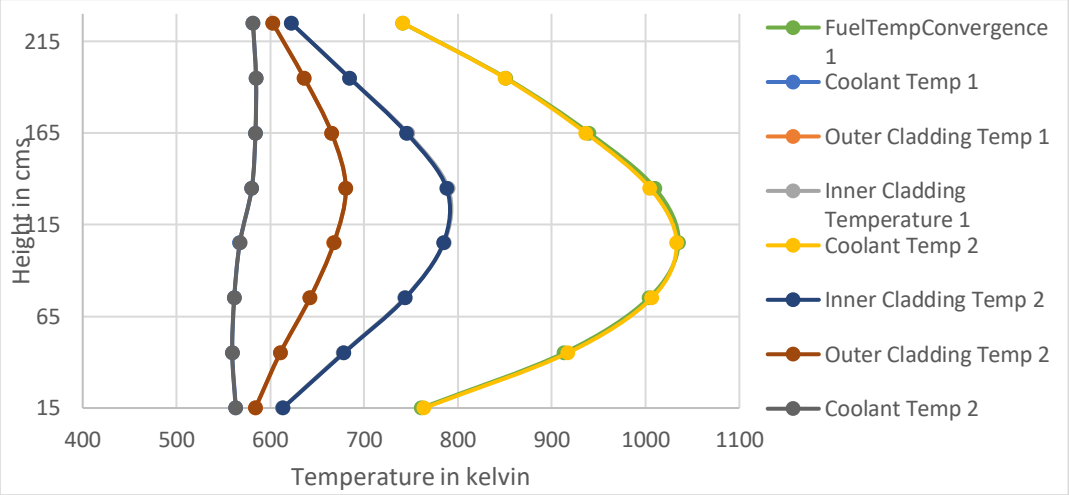

5.2 Xenon Stability Results

During this research, the reactor is expected to go through four main phases. The first phase is essentially the period of time before the control rod removal. In this phase, the xenon concentration is rapidly building up to the equilibrium levels for the neutron flux levels associated with the power conditions. The next phase or "rod removal" phase is the period of time during which the control rod is removed and maintained in the top region of the core. The control rod removal results in an instantaneous change in the shape of the flux by increasing the flux in the bottom region of the core. Due to the constant power requirement, the power in the bottom region of the core increases to compensate for the decreased power production in the top region of the core. The xenon stability is measured in a "free oscillation mode" meaning that no control actions are taken to dampen the oscillation [18]. The final phase is the "return to equilibrium" phase.

Depending on the xenon stability of the core, a new equilibrium xenon distribution will be achieved after a few oscillation periods. If the core is inherently unstable, the return to equilibrium phase is not achieved in the free oscillation mode and control rod movement is required to regain control of core power.

Removal of the control rod initiates the oscillation phase; characterized by the fluctuation of majority power production between the two regions of the core. This phase appears to persist for nearly thirty hours before returning to equilibrium.

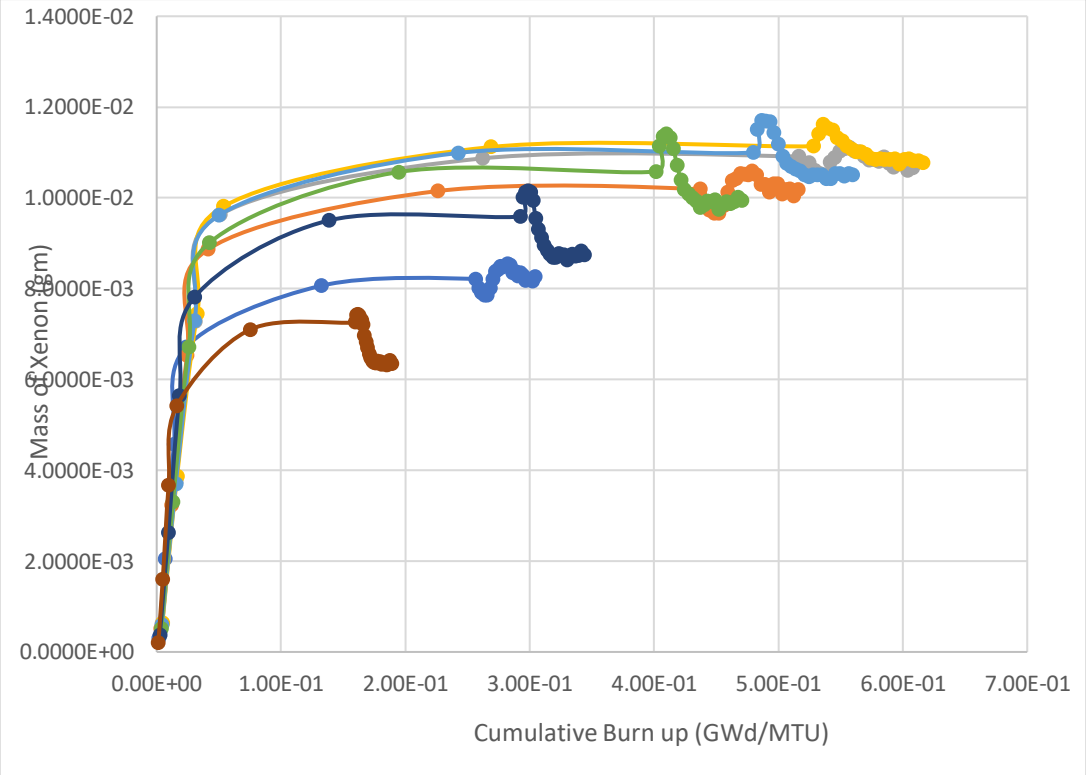

Figure 21: Buildup of Xenon mass with cumulative burn up of the fuel in SMR core

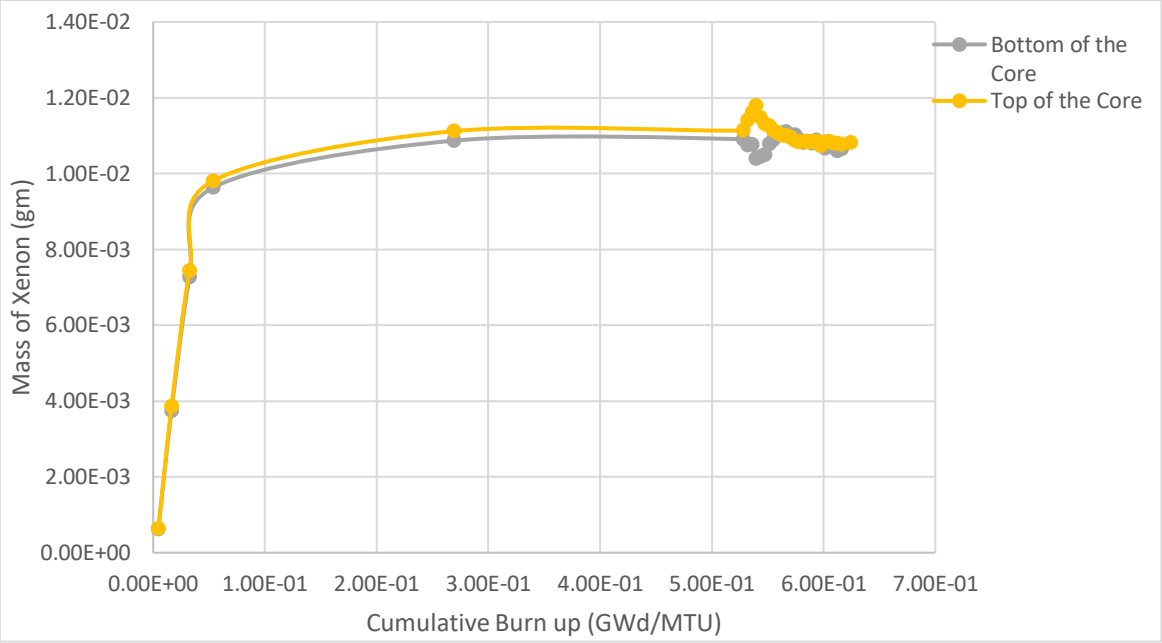

Figure 22: Xenon Oscillatory behavior with removal of control rod

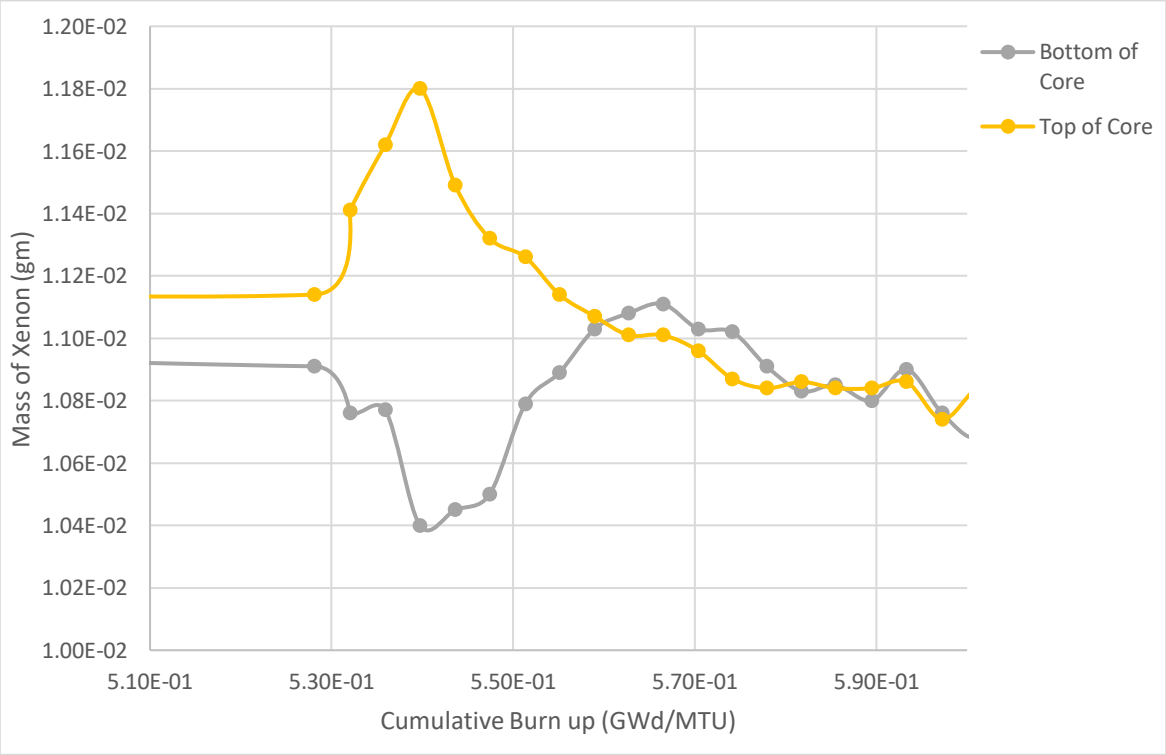

Figure 23: Xenon Oscillatory behavior with the Control Rod Movement

Oscillation is induced with control rod withdrawal from the bottom of the core which leads to local increase of neutron flux and Xe-135 burnup at the bottom. With increased flux at the bottom, increased I-135 production starts. I-135 then decays back to Xe-135 with some delay, causing Xe-135 concentrations to rise at the bottom (Figure 24; yellow curve) and decline at the top (Figure 24; grey curve). When profiles eventually reverse, process repeats with the opposite phase, causing Xe-135 concentrations to slowly follow the neutron flux profile and thus leading to initial perturbation. Thus, the neutron reactivity change in one region of the core will result in a decreased thermal neutron flux and a higher Xe-135 concentration while the other region will have a higher thermal neutron flux and lower Xe-135 concentration. As described, processes rely primarily on I-135 decay, period of xenon oscillations is in the order of magnitude of I-135 half life. The nature and stability of oscillations depend heavily on the initial perturbation to the neutron flux, reactor design and its operating conditions.

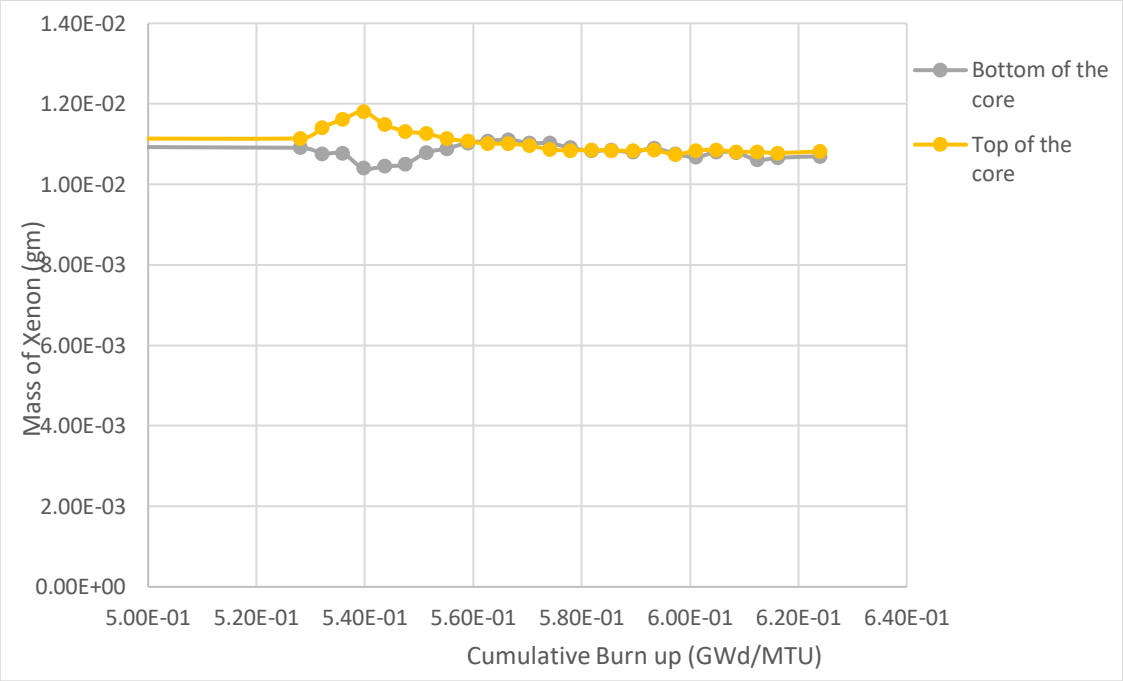

Figure 24: Xenon Oscillations with Cumulative Burn up

CHAPTER VI

CONCLUSION

The goal of this research was to develop a multi-physics methodology whereby high-fidelity reactor physics simulations could be performed to observe the xenon oscillatory behavior, if any, due to transients in a small modular reactor if the *i*PWR-type. The methodology using MCNP as the neutronics solver was applied to a generic SMR core performing thermal hydraulic analysis and performance assessments as well as observing the xenon oscillatory behavior in the SMR. This section provides a detailed summary of the research along with conclusions of the SMR core model and discusses possible avenues for future research.

7.1 Research Summary

The multi-physics coupling computational methodology developed was initialized with the MCNP model of the SMR at steady state conditions and fuel depletion simulations were performed. Using the SCA tool developed in Python, the power fractions were parsed from the simulations. to the SCA. Fuel and coolant temperature distributions were calculated using appropriate material compositions of the fuel based on temperature dependent cross sections, the xenon oscillatory behavior was studied using the appropriate Doppler broadened neutron cross sections by the weighted fractions of fuel.

The SMR core model was developed in MCNP6 with the proposed performance characteristics of the B&W mPower reactor design. The resulting SMR featured sixty-

nine fuel assemblies with an active fuel length of 240 centimeters producing 530 MW of thermal power with a core refueling time of four years. The fuel enrichment was limited to below five percent uranium-235. Burnable absorber rods (BARs) with boron carbide as the absorber material were used. The fidelity of the model was increased by adding eight axial regions within each fuel geometry and accompanying coolant segments within the coolant. To reduce the computational time for the fuel depletion simulations only one-eighth of the core was modelled. The final simulation model featured thirteen assemblies each with eight axial fuel regions for a total of 104 fuel regions, 104 coolant regions.

Axial neutron flux, fuel and coolant temperature, and xenon mass distributions are shown to evolve as expected in LEU light-water systems. The effective neutron multiplication factor decreased rapidly in the as fission products build up and due to the temperature-dependent doppler broadened neutron cross-section in fresh fuel. Convergence of neutron flux and reaction rate tallies were studied, and the results were converged. In conclusion, a multi-physics analysis methodology was developed and utilized to assess a generic SMR core design. The design is found to be inherently stable and xenon oscillatory behavior was studied. Xenon oscillations were as expected in a LEU light water system with the modelling and execution of MCNP6.

7.2 Future Research

The multi-physics methodology developed allows for the simulation of complex, time-dependent reactor design problems with temperature feedback mechanisms by coupling existing state-of-the-art codes using an external coupling script. This

methodology was applied to the safety and performance assessment of a generic SMR. Future research could focus on multi-channel analysis with respect to , the thermal hydraulic assessment taking into consideration their cross influences. Hence, coupling to existing state-of-the-art thermal hydraulics tools such as RELAP-3D or the use of computational fluid dynamics (CFD) should be explored.

Another area for further research will be to explore the components of the balance of plant and optimize further feedback mechanisms. Thus, it is unlikely that *i*PWR SMRs of a similar design will experience disruptions in operations due to xenon-induced power oscillations.

REFERENCES

[1] W. C. J, "MCNP Users Manual-Code Version 6.2," *Los Alamos National Laboratory,* 2017.

[2] "World nuclear assosiation; world energy needs and nuclear power," october 2010. [Online]. Available: https://www.world-nuclear.org/information-library/current-and-future-generation/world-energy-needs-and-nuclear-power.aspx.

[3] G. G. M. M.D. Carellia, "Economic features of integral, modular, small to medium size reactors.," pp. 403- 414, May 2010.

[4] F. B. G. J. T. &. S. J. E. Brown, "Proceedings of ANS Mathematics & Computation Topical Meeting," in *MCNP5 Parallel Processing Workshop*, Gatlinburg, 2003.

[5] I. D. T, "Deliberately Small Reactors and the Second Nuclear Era.," *Progress in Nuclear Energy,* pp. 51 (4-5), 589-603, 2009.

[6] E. D. Kitcher, *Performance and Safety Analyis of a Generic Small Modular Reactor,* Ph.D. Dissertation; Texas A&M University, 2012.

[7] W. R. M. Forrest B. Brown, "Monte Carlo - Advances and Challenges," *Workshop at PHYSOR-2008*, pp. 14-19 , 2008.

[8] I. A. E. Agency, "Small Modular Reactors," [Online]. Available: https://www.iaea.org/topics/small-modular-reactors.

[9] NRC, "mPower Reactor Design Overview Workshop Slides - NRC," 21 april 2011. [Online]. Available: https://www.nrc.gov/docs/ML1110/ML11102A097.pdf.

[10] U. S. N. R. Commision, "Advanced Reactors and Small Modular Reactors-Holtec," United States Nuclear Regualtory Commision, 14 September 2015. [Online]. Available: http://www.nrc.gov/reactors/advanced/holtec.html.

[11] "Advanced Reactors and Small Modular Reactors- NuScale," United States Nuclear Regulatory Commision , 14 September 2014. [Online]. Available: https://www.nrc.gov/reactors/new-reactors/smr/nuscale.html.

[12] "Advanced Reactors and Small Modular Reactors," United States Nuclear Regualtory Commision, 14 September 2015. [Online]. Available: https://www.westinghousenuclear.com/new-plants/small-modular-reactor#:~:text=The%20Westinghouse%20SMR%20is%20a,located%20inside%20the%20reactor%20vessel.&text=This%20approach%20will%20provide%20licensing,other%20SMR%20supplier%20can%20match..

[13] "Advanced Reactors and Small Modular Reactors," United States Nuclear Regulatory Commision, 14 September 2015. [Online]. Available: http://www.nrc.gov/reactors/advanced/mpower.html.

[14] R. J. Onega and R. A. Kisner, "An Axial Xenon Oscillation Model," *Annals of Nuclear Energy,* pp. 13-19, 1978.

[15] S. W. M, Nuclear Reactor Physics, John Wiley and Sons, 2007.

[16] J. R. Lamarsh, Introduction to nuclear reactor theory, Addison, 1972.

[17] B. Zajec, "Xenon Oscillations," University of Ljubljana, 2017.

[18] R. P. L, "The Influence of Xenon-135 on Reactor Operation," *Aiken: WSRC,* 2000.

[19] L. A. F. M.-F. Miriam Vazquez, "Coupled neutronics thermal-hydraulics analysis using Monte Carlo and sub-channel codes," *Nuclear Engineering and Design,* vol. 250, pp. 403-411, 2012.

[20] J. W. L. S. Tong, Thermal Analysis of Pressurized Water Reactors, 1996.

[21] E. T. R, "CINDER - A One Point Depletion and Fission Product Program," Westinghouse Electric Corp. Bettis Atomic Power Lab, Pittsburgh, 1962.

[22] W. B. E. T. R. A. E. D. B. C. A. &. B. C. D. Wilson, "Accelerator Transmutation Studies at Los Alamos with LAHET, MCNP, and CINDER 90," Los Alamos National Lab, Los Alamos, 1993.

[23] W. C. S. E. T. R. H. A. &. M. P. Wilson, "A manual for CINDER 90 version 07.4 codes and data," Los Alamos National Lab, Los Alamos, 2007.

[24] " Acceptance criteria for emergency core cooling systems for light water nuclear power reactors, As amended at 72 FR 49508,," Code of Federal Regulations. 10CFR50.46., August 2007.

[25] J. G. &. T. J. R. Collier, " Convective Boiling and Condensation," vol. Oxford: Clarendon Press., 1972.

[26] "International Association for the Properties of Water and Steam; Revised release on the IAPWS industrial formulation 1997 for the Thermodynamic properties of water and steam," IAPWS, Lucerne, 2007.

[27] H. P. K. M. Shirvan K., " The Design of a Compact Integral Medium Size PWR," *Nuclear Engineering Design*, pp. 393-403 , 2012.

[28] "National Historic Mechanical Engineering Hanford B. Reactor, Richland," *American Society of Mechanical Engineers,* 1976.

[29] M. B. B.Pershagen, "Light water reactor safety," 2013.

[30] S. W. M, "Xenon-induced Spatial Power Oscillations. Reactor Technology," pp. 13 (3), 252-279, 1970.

[31] J. C. W. R. B. W. &. L. L. K. Shan, "Coupled neutronics/thermal hydraulics analysis of CANDU-SCWR Fuel channel," *Annals of Nuclear Energy*, pp. 37(1), 58-65., 2010.

[32] K. D. Kok, Nuclear Engineering Handbook, Boca Raton, Florida: CRC Press, 2009.

[33] D. Pelowitz, "MCNPX User's Manual Version 2.6.0.," Los Alamos National Laboratory, Los Alamos, 2008.

.